We are IntechOpen, the world's leading publisher of Open Access books Built by scientists, for scientists

4,800
Open access books available

122,000
International authors and editors

135M
Downloads

Our authors are among the

154
Countries delivered to

TOP 1%
most cited scientists

12.2%
Contributors from top 500 universities

CLARIVATE ANALYTICS BOOK CITATION INDEX INDEXED

WEB OF SCIENCE™

Selection of our books indexed in the Book Citation Index in Web of Science™ Core Collection (BKCI)

Interested in publishing with us?
Contact book.department@intechopen.com

Numbers displayed above are based on latest data collected.
For more information visit www.intechopen.com

15

A General Approach to Discrete-Time Adaptive Control Systems with Perturbed Measures for Complex Dynamics - Case Study: Unmanned Underwater Vehicles

Mario Alberto Jordán and Jorge Luis Bustamante
Argentine Institute of Oceanography (IADO-CONICET) and Department of Electrical Engineering and Computers, National University of the South (DIEC-UNS), Florida 8000, B8000FWB Bahía Blanca
Argentina

1. Introduction

New design tools and systematic design procedures has been developed in the past decade to adaptive control for a set of general classes of nonlinear systems with uncertainties (Krstić et al., 1995; Fradkov et al., 1999). In the absence of modeling uncertainties, adaptive controllers can achieve in general global boundness, asymptotic tracking, passivity of the adaptation loop and systematic improvement of transient performance. Also, other sources of uncertainty like intrinsic disturbances acting on measures and exogenous perturbations are taking into account in many approaches in order for the controllers to be more robust.

The development of adaptive guidance systems for unmanned vehicles is recently starting to gain in interest in different application fields like autonomous vehicles in aerial, terrestrial as well as in subaquatic environments (Antonelli, 2007; Sun & Cheah, 2003; Kahveci et al., 2008; Bagnell et al., 2010). These complex dynamics involve a high degree of uncertainty (specially in the case of underwater vehicles), namely located in the inertia, added mass, Coriolis and centripetal forces, buoyancy and linear and nonlinear damping.

When applying digital technology, both in computing and communication, the implementation of controllers in digital form is unavoidable. This fact is strengthened by many applications where the sensorial components work inherently digitally at regular periods of time. However, usual applications in path tracking of unmanned vehicles are characterized by analog control approaches (Fossen, 1994; Inzartev, 2009).

The translation of existing analog-controller design approaches to the discrete-time domain is commonly done by a simple digitalization of the controlling action, and in the case of adaptive controllers, of the adaptive laws too (Cunha et al., 1995; Smallwood & Whitcomb, 2003). This way generally provides a good control system behavior. However the role played by the sampling time in the stability and performance must be cautiously investigated. Additionally, noisy measures and digitalization errors may not only affect the stability properties significantly but also increase the complexity of the analysis even for the simplest

approaches based on Euler or Tustin discretization methods (Jordán & Bustamante, 2009a; Jordán & Bustamante, 2009b; Jordán et al., 2010).
On the other side, controller designs being carried out directly in the discrete-time domain seem to be a more promising alternative than the translation approaches. This is sustained on the fact that model errors as well as perturbations are included in the design approach directly to ensure stability and performance specifications.
This work is concerned about a novel design of discrete-time adaptive controllers for path tracking of unmanned underwater vehicles subject to perturbations and measure disturbances. The presented approach is completely developed in the discrete time domain. Formal proofs are presented for stability and performance. Finally, a case study related to a complex guidance system in 6 degrees of freedom (DOF´s) is worked through to illustrate the features of the proposed approach.

2. Notation

Throughout the chapter, vectors are denoted in lower case and bold letters, scalars in lower case letters, matrices in capital letters. A function dependence on a variable is denoted with brackets as for instance $F[x]$. Also brackets are employed to enclose the elements of a vector. Elements of a set are described as enclosed in braces. Parentheses are only used to separate factors with terms of an expression. Subscripts are applied to reference elements in sequences, in matrices or sample-time points. In time sequences, one will distinguish between a prediction x_{n+1} at time t_n from a sample $x[t_n] = x_{t_n}$ at sample time t_n. Often we apply the notation for a derivative of a scalar function with respect to a quadratic matrix, meaning a new matrix with elements describing the derivative of the scalar function with respect to each element of the original matrix. For instance: let the functional Q be depending on the elements x_{ij} of the matrix X in the form $Q = (MX\mathbf{v}_1)^T \mathbf{v}_2$, then it has a derivative $\partial Q/\partial X = M^T \mathbf{v}_2 \mathbf{v}_1^T$. Finally we will also make reference to $\partial Q/\partial \mathbf{x}_j$ meaning a gradient vector of the functional Q with respect to the vector $\mathbf{x}_j$, being this the column j of X.

3. Vehicle dynamics

3.1 Physical dynamics from ODEs

Many systems are described as the conjugation of two ODEs in generalized variables, namely one for the kinematics and the other one for the inertia (see Fig. 1). The block structure embraces a wide range of vehicle systems like mobile robots, unmanned aerial vehicles (UAV), spacecraft and satellite systems, autonomous underwater vehicles (AUV) and remotely operated vehicles (ROV), though with slight distinctive modifications in the structure among them.
Let $\boldsymbol{\eta} = [x, y, z, \varphi, \theta, \psi]^T$ be the generalized position vector referred on a earth-fixed coordinate system termed O', with displacements x, y, z, and rotation angles φ, θ, ψ about these directions, respectively. The motions associated to the elements of $\boldsymbol{\eta}$ are referred to as surge, sway, heave, roll, pitch and yaw, respectively.
Additionally let $\mathbf{v} = [u, v, w, p, q, r]^T$ be the generalized rate vector referred on a vehicle-fixed coordinate system termed O, oriented according to their main axes with translation rates u, v, w and angular rates p, q, r about these directions, respectively.

The vehicle dynamics is described as (see Jordán & Bustamante, 2009c; cf. Fossen, 1994)

$$\dot{\mathbf{v}}=M^{-1}\left(-C[\mathbf{v}]\mathbf{v}-D[|\mathbf{v}|]\mathbf{v}-\mathbf{g}[\boldsymbol{\eta}]+\boldsymbol{\tau}_c+\boldsymbol{\tau}\right) \tag{1}$$

$$\dot{\boldsymbol{\eta}}=J[\boldsymbol{\eta}](\mathbf{v}+\mathbf{v}_c). \tag{2}$$

Here M, C and D are the inertia, the Coriolis-centripetal and the drag matrices, respectively and J is the matrix expressing the transformation from the inertial frame to the vehicle-fixed frame. Moreover, $\mathbf{g}$ is the restoration force due to buoyancy and weight, $\boldsymbol{\tau}$ is the generalized propulsion force (also the future control action of a controller), $\boldsymbol{\tau}_c$ is a generalized perturbation force (for instance due to wind as in case of UAVs, fluid flow in AUVs, or cable tugs in ROVs) and $\mathbf{v}_c$ is a velocity perturbation (for instance the fluid current in ROVs/AUVs or wind rate in UAVs), all of them applied to O.
Also disturbances acting on the measures are indicated as $\delta\boldsymbol{\eta}$ and $\delta\mathbf{v}$, while noisy measures are referred to as $\boldsymbol{\eta}_\delta$ and $\mathbf{v}_\delta$, respectively.
Particularly, in fluid environment the mass is broken down into

$$M = M_b + M_a, \tag{3}$$

with M_b body mass matrix, M_a the additive mass matrix related to the dragged fluid mass in the surroundings of the moving vehicle.
For future developments in the controller design, it is convenient to factorize the system matrices into constant and variable arrays as (Jordán & Bustamante, 2009c)

$$C[\mathbf{v}] = \sum_{i=1}^{6} C_i. \times C_{v_i}[\mathbf{v}] \tag{4}$$

$$D[|\mathbf{v}|] = D_l + \sum_{i=1}^{6} D_{q_i}\,|v_i| \tag{5}$$

$$\mathbf{g}[\boldsymbol{\eta}] = B_1\,\mathbf{g}_1[\boldsymbol{\eta}]+B_2\mathbf{g}_2[\boldsymbol{\eta}], \tag{6}$$

with ".×" being an element-by-element array product. The matrices C_i, D_l, D_{q_i}, B_1 and B_2 are constant and supposed unknown, while C_{v_i}, $\mathbf{g}_1$ and $\mathbf{g}_2$ are state-dependent and computable arrays and v_i is an element of $\mathbf{v}$.
The generalized propulsion force $\boldsymbol{\tau}$ applied on O is broken down into force components provided by each thruster. These components termed f_i are arranged in the vector $\mathbf{f}$ which obeys the relation

$$\mathbf{f}=B^T\left(BB^T\right)^{-1}\boldsymbol{\tau}, \tag{7}$$

with B a commonly rectangular matrix that expresses the transformation of $\boldsymbol{\tau}$ into these thrust components.
On the other hand, $\mathbf{f}$ is related to a strong nonlinear characteristic which is proper of each thruster. Specially for underwater vehicles this is modelled by (cf. Fossen, 1994)

$$\mathbf{f}=K_1\left(|\mathbf{n}|\,.\mathbf{n}\right)-K_2\left(|\mathbf{n}|\,.\mathbf{v}_\mathrm{a}\right), \tag{8}$$

where K_1 and K_2 are constant matrices accounting for the influence of the thruster angular velocity $\mathbf{n}$ and the state $\mathbf{v}_\mathrm{a}$ related to every thruster force component in $\mathbf{f}$.

The thruster dynamics usually corresponds to a controlled system with input $\mathbf{n}_{ref}$ and output $\mathbf{n}$ given generally by a linear dynamics indicated generically as some linear vector funcion $\mathbf{k}$ in Laplace variable form

$$\mathbf{n}=\mathbf{k}[\mathbf{n}_{ref},\mathbf{v}], \tag{9}$$

where $\mathbf{n}_{ref}$ is the reference angular velocity referred to as the real input of the vehicle dynamics.

Usually in the literature it is assumed that the rapid thruster dynamics is parasitic in comparison with the dominant vehicle dynamics. In the same way we will neglect this parasitics and so the equality $\mathbf{n}=\mathbf{n}_{ref}$ will be employed throughout the chapter.

Moreover, we will concentrate henceforth on disturbed measures $\boldsymbol{\eta}_\delta$ and $\mathbf{v}_\delta$, and not on exogenous perturbations $\boldsymbol{\tau}_c$ and $\mathbf{v}_c$, so we have set $\boldsymbol{\tau}_c=\mathbf{v}_c=0$ throughout the paper. Similarly, $\mathbf{v}=\bar{\mathbf{v}}$ and $\boldsymbol{\eta}=\bar{\boldsymbol{\eta}}$ (see Fig. 1). For details of the influence of $\boldsymbol{\tau}_c$ and $\mathbf{v}_c$ on adaptive guidance systems see (Jordán and Bustamante, 2008; Jordán and Bustamante 2007), respectively.

3.2 Sampled-data behavior

For the continuous-time dynamics there exists an associated exact sampled-data dynamics described by the set of sequences $\{\boldsymbol{\eta}[t_i],\mathbf{v}[t_i]\}=\left\{\boldsymbol{\eta}_{t_i},\mathbf{v}_{t_i}\right\}$ for the states $\boldsymbol{\eta}[t]$ and $\mathbf{v}[t]$ at sample times t_i with a sampling rate h.

On the other side, we let the sampled measures for the kinematics and positioning state vectors be disturbed. So this is characterized in discrete time through the noisy measurements in the sequence set $\{\boldsymbol{\eta}_\delta[t_i],\mathbf{v}_\delta[t_i]\}=\left\{\boldsymbol{\eta}_{\delta_{t_i}},\mathbf{v}_{\delta_{t_i}}\right\}$ as illustrated in Fig. 1.

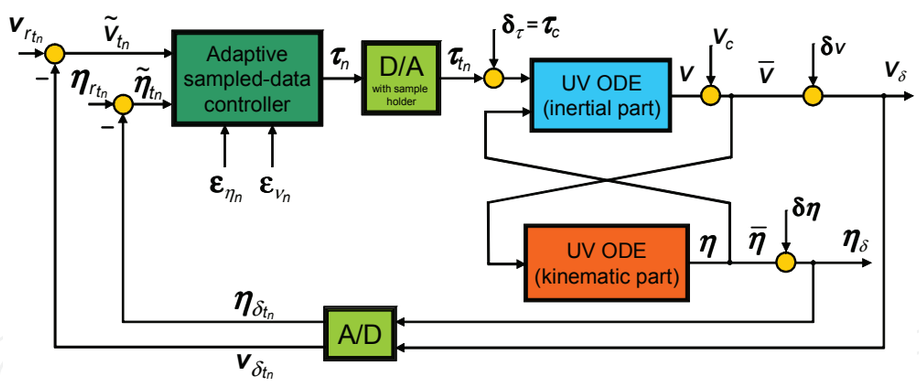

Fig. 1. Adaptive digital control system for underwater vehicles (UV) with noisy measures, model errors and exogenous perturbations

3.3 Sampled-data model

Usually, sampled-data behavior can be modelled by n-steps-ahead predictors (Jordán & Bustamante, 2009a). Accordingly, we attempt now to translate the continuous time dynamics of the system into a discrete-time model. The ODEs in (1)-(2) can be described in a compact form by

$$\dot{\mathbf{v}} = M^{-1}\mathbf{p}[\boldsymbol{\eta},\mathbf{v}]+M^{-1}\boldsymbol{\tau} \tag{10}$$

$$\dot{\boldsymbol{\eta}} = \mathbf{q}[\boldsymbol{\eta},\mathbf{v}], \tag{11}$$

with $\mathbf{p}$ and $\mathbf{q}$ being Lipschitz vector functions located at the right-hand memberships of (1) and (2), respectively. Here no exogenous perturbation was considered as agreed above.
Let us contemplate an approximation of first order of an Adams-Bashforth approximator (Jordán & Bustamante, 2009b). It is valid

$$\mathbf{v}_{n+1} = \mathbf{v}_{t_n} + hM^{-1}\left(\mathbf{p}_{\delta_{t_n}} + \boldsymbol{\tau}_n\right) \tag{12}$$

$$\boldsymbol{\eta}_{n+1} = \boldsymbol{\eta}_{t_n} + h\mathbf{q}_{t_n}, \tag{13}$$

where $\boldsymbol{\eta}_{n+1}$ and $\mathbf{v}_{n+1}$ are one-step-ahead predictions at the present time t_n. Moreover, $\boldsymbol{\tau}_n$ is the discrete-time control action at t_n, which is equal to the sample $\boldsymbol{\tau}[t_n]$ because of the employed zero-order sample holder.
More precisely it is valid with (1)-(2)

$$\mathbf{p}_{t_n} = -\sum_{i=1}^{6} C_i. \times C_{v_{i_{t_n}}} \mathbf{v}_{t_n} - D_l \mathbf{v}_{t_n} - \tag{14}$$

$$-\sum_{i=1}^{6} D_{q_i} \, |v_{i_{t_n}}| \mathbf{v}_{t_n} - B_1 \, \mathbf{g}_{1_{t_n}} - B_2 \, \mathbf{g}_{2_{t_n}}$$

$$\mathbf{q}_{t_n} = J_{t_n} \mathbf{v}_{t_n} \tag{15}$$

where $C_{v_{i_{t_n}}}$ means $C_{v_i}[\mathbf{v}_{t_n}]$, $\mathbf{g}_{1_{t_n}}$ and $\mathbf{g}_{2_{t_n}}$ mean $\mathbf{g}_1[\boldsymbol{\eta}_{t_n}]$ and $\mathbf{g}_2[\boldsymbol{\eta}_{t_n}]$ respectively, $J_{t_n}^{-1}$ means $J^{-1}[\boldsymbol{\eta}_{t_n}]$ and $v_{i_{t_n}}$ is an element of $\mathbf{v}_{t_n}$. Similar expressions can be obtained for the other sampled functions $\mathbf{p}_{t_i}$ and $\mathbf{q}_{t_i}$ in (18)-(19). Besides, the control action $\boldsymbol{\tau}$ is retained one sampling period h by a sample holder, so it is valid $\boldsymbol{\tau}_n = \boldsymbol{\tau}_{t_n}$.
The accuracy of one-step-ahead predictions is defined by the local model errors as

$$\boldsymbol{\varepsilon}_{v_{n+1}} = \mathbf{v}_{t_{n+1}} - \mathbf{v}_{n+1} \tag{16}$$

$$\boldsymbol{\varepsilon}_{\eta_{n+1}} = \boldsymbol{\eta}_{t_{n+1}} - \boldsymbol{\eta}_{n+1}, \tag{17}$$

with $\boldsymbol{\varepsilon}_{\eta_{n+1}}$, $\boldsymbol{\varepsilon}_{v_{n+1}} \in \mathcal{O}[h]$ and $\mathcal{O}$ being the order function that expresses the order of magnitude of the sampled-data model errors. It is noticing that local errors are by definition completely lacking of the influence from sampled-data disturbances.
Since $\mathbf{p}$ and $\mathbf{q}$ are Lipschitz continuous in the attraction domains in $\mathbf{v}$ and $\boldsymbol{\eta}$, then the samples, predictions and local errors all yield bounded. So it is valid the property $\mathbf{v}_{n+1} \to \mathbf{v}_{t_{n+1}}$ and $\boldsymbol{\eta}_{n+1} \to \boldsymbol{\eta}_{t_{n+1}}$ for $h \to 0$.
Next, the disturbed dynamics subject to sampled-data noisy measures is dealt with in the following.

3.4 1st-order predictor with disturbances

The one-step-ahead predictions with disturbances result from (18) and (19) as

$$\mathbf{v}_{n+1} = \mathbf{v}_{t_n} + \delta\mathbf{v}_{t_n} + hM^{-1}\left(\mathbf{p}_{\delta_{t_n}} + \boldsymbol{\tau}_n\right) \tag{18}$$

$$\boldsymbol{\eta}_{n+1} = \boldsymbol{\eta}_{t_n} + \delta\boldsymbol{\eta}_{t_n} + h\mathbf{q}_{\delta_{t_n}}, \tag{19}$$

where $\mathbf{v}_{t_n}+\delta\mathbf{v}_{t_n}=\mathbf{v}_{\delta_{t_n}}$ and $\boldsymbol{\eta}_{t_n}+\delta\boldsymbol{\eta}_{t_n}=\boldsymbol{\eta}_{\delta_{t_n}}$ are samples of the measure disturbances (see Fig. 1), and $\mathbf{p}_{\delta_{t_n}}$ and $\mathbf{q}_{\delta_{t_n}}$ are perturbed functions defined as $\mathbf{p}_{\delta_{t_n}}=\mathbf{p}\left[\mathbf{v}_{t_n}+\delta\mathbf{v}_{t_n},\boldsymbol{\eta}_{t_n}+\delta\boldsymbol{\eta}_{t_n}\right]$ and $\mathbf{q}_{\delta_{t_n}}=\mathbf{q}\left[\mathbf{v}_{t_n}+\delta\mathbf{v}_{t_n},\boldsymbol{\eta}_{t_n}+\delta\boldsymbol{\eta}_{t_n}\right]$.

3.5 Disturbed local error

Assuming bounded noise vectors $\delta\mathbf{v}_i$ and $\delta\boldsymbol{\eta}_i$, we can expand (18) and (19) in series of Taylor about the values of undisturbed measures $\mathbf{v}[t_n]$ and $\boldsymbol{\eta}[t_n]$. So it is accomplished

$$\begin{aligned}\bar{\boldsymbol{\varepsilon}}_{v_{n+1}} &= \boldsymbol{\varepsilon}_{v_{n+1}}+\Delta\delta\mathbf{v}_{t_{n+1}}-hM^{-1}\left(\frac{\partial\mathbf{p}_\delta^T}{\partial\mathbf{v}}\delta\mathbf{v}_{t_n}+\frac{\partial\mathbf{p}_\delta^T}{\partial\boldsymbol{\eta}}[t_n]\delta\boldsymbol{\eta}_{t_n}+\right.\\ &\left.+\frac{\partial\boldsymbol{\tau}_n^T}{\partial\mathbf{v}}\delta\mathbf{v}_{t_n}+\frac{\partial\boldsymbol{\tau}_n^T}{\partial\boldsymbol{\eta}}\delta\boldsymbol{\eta}_{t_n}+\mathbf{o}[\delta\mathbf{v}^2]+\mathbf{o}[\delta\boldsymbol{\eta}^2]\right) \qquad (20)\\ \bar{\boldsymbol{\varepsilon}}_{\eta_{n+1}} &= \boldsymbol{\varepsilon}_{\eta_{n+1}}+\Delta\delta\boldsymbol{\eta}_{t_{n+1}}-h\left(\frac{\partial\mathbf{q}_\delta^T}{\partial\mathbf{v}}[t_n]\delta\mathbf{v}_{t_n}+\right.\\ &\left.+\frac{\partial\mathbf{q}_\delta^T}{\partial\boldsymbol{\eta}}[t_n]\delta\boldsymbol{\eta}_{t_n}+\mathbf{o}[\delta\mathbf{v}^2]+\mathbf{o}[\delta\boldsymbol{\eta}^2]\right), \qquad (21)\end{aligned}$$

where $\boldsymbol{\varepsilon}_{v_{n+1}}$ and $\boldsymbol{\varepsilon}_{\eta_{n+1}}$ are the model local errors and $\Delta\delta\mathbf{v}_{t_{n+1}}=\delta\mathbf{v}_{t_{n+1}}-\delta\mathbf{v}_{t_n}$ and $\Delta\delta\boldsymbol{\eta}_{t_{n+1}}=\delta\boldsymbol{\eta}_{t_{n+1}}-\delta\boldsymbol{\eta}_{t_n}$. The functions $\mathbf{o}$ are truncating error vectors of the Taylor series expansions, all of them belonging to $\mathcal{O}[h^2]$. Moreover, $\frac{\partial\mathbf{p}_\delta^T}{\partial\mathbf{v}}$, $\frac{\partial\mathbf{p}_\delta^T}{\partial\boldsymbol{\eta}}$, $\frac{\partial\mathbf{q}_\delta^T}{\partial\mathbf{v}}$ and $\frac{\partial\mathbf{q}_\delta^T}{\partial\boldsymbol{\eta}}$ are Jacobian matrices of the system which act as variable gains that strengthen the sampled-data disturbances along the path.

It is worth noticing that the Jacobian matrices $\frac{\partial\boldsymbol{\tau}_n^T}{\partial\mathbf{v}}$ and $\frac{\partial\boldsymbol{\tau}_n^T}{\partial\boldsymbol{\eta}}$ in (20) will be obtained from the feedback law $\boldsymbol{\tau}_n[\bar{\boldsymbol{\eta}}_{t_n},\bar{\mathbf{v}}_{t_n}]$ of the adaptive control loop.

4. Sampled-data adaptive controller

The next step is devoted to the stability and performance study of a general class of adaptive control systems whose state feedback law is constructed from noisy measures and model errors.

A design of a general completely adaptive digital controller based on speed-gradient control laws is presented in (Jordán & Bustamante, 2011). To this end let us suppose the control goal lies on the path tracking of both geometric and kinematic reference as $\boldsymbol{\eta}_{r_{t_n}}$ and $\mathbf{v}_{r_{t_n}}$, respectively.

4.1 Control action

Accordingly to the digital model translation, we try out the following definitions for the exact path errors

$$\begin{aligned}\overset{\frown}{\boldsymbol{\eta}}_{t_n} &= \boldsymbol{\eta}_{t_n}+\delta\boldsymbol{\eta}_{t_n}-\boldsymbol{\eta}_{r_{t_n}} \qquad (22)\\ \overset{\frown}{\mathbf{v}}_{t_n} &= \mathbf{v}_{t_n}+\delta\mathbf{v}_{t_n}-J_{\delta_{t_n}}^{-1}\dot{\boldsymbol{\eta}}_{r_{t_n}}+J_{\delta_{t_n}}^{-1}K_p\overset{\frown}{\boldsymbol{\eta}}_{t_n}. \qquad (23)\end{aligned}$$

where $K_p = K_p^T \geq 0$ is a design gain matrix affecting the geometric path error and $J_{\delta_{t_n}}^{-1}$ means $J^{-1}[\boldsymbol{\eta}_{t_n}+\delta\boldsymbol{\eta}_{t_n}]$. Clearly, if $\breve{\boldsymbol{\eta}}_{t_n}\equiv\mathbf{0}$, then by (23) and (2), it yields $\mathbf{v}_{t_n}+\delta\mathbf{v}_{t_n}-\mathbf{v}_{r_{t_n}}\equiv\mathbf{0}$.
Then, replacing (18) and (19) in (22) for t_{n+1} one gets

$$\begin{aligned}\breve{\boldsymbol{\eta}}_{t_{n+1}} = &\left(I - hJ_{t_n}J_{\delta_{t_n}}^{-1}K_p\right)\breve{\boldsymbol{\eta}}_{t_n}+\boldsymbol{\eta}_{r_{t_n}}-\boldsymbol{\eta}_{r_{t_{n+1}}}+\delta\boldsymbol{\eta}_{t_{n+1}}-\delta\boldsymbol{\eta}_{t_n} \\ &+\boldsymbol{\varepsilon}_{\eta_{n+1}}+h\left(J_{t_n}\breve{\mathbf{v}}_{t_n}+J_{t_n}\delta\mathbf{v}_{t_n}+J_{t_n}J_{\delta_{t_n}}^{-1}\dot{\boldsymbol{\eta}}_{r_{t_n}}\right).\end{aligned} \tag{24}$$

Similarly, with (18) and (19) in (23) for t_{n+1} one obtains

$$\begin{aligned}\breve{\mathbf{v}}_{t_{n+1}} = &\breve{\mathbf{v}}_{t_n}+J_{\delta_{t_n}}^{-1}\dot{\boldsymbol{\eta}}_{r_{t_n}}-J_{\delta_{t_{n+1}}}^{-1}\dot{\boldsymbol{\eta}}_{r_{t_{n+1}}}-J_{\delta_{t_n}}^{-1}K_p\breve{\boldsymbol{\eta}}_{t_n}+ \\ &+J_{\delta_{t_{n+1}}}^{-1}K_p\breve{\boldsymbol{\eta}}_{t_{n+1}}+\boldsymbol{\varepsilon}_{v_{n+1}}+\delta\mathbf{v}_{t_{n+1}}-\delta\mathbf{v}_{t_n}+hM^{-1}\left(\mathbf{p}_{\delta_{t_n}}+\boldsymbol{\tau}_n\right).\end{aligned} \tag{25}$$

We now define a cost functional of the path error energy as

$$Q_{t_n} = \breve{\boldsymbol{\eta}}_{t_n}^T\breve{\boldsymbol{\eta}}_{t_n}+\breve{\mathbf{v}}_{t_n}^T\breve{\mathbf{v}}_{t_n}, \tag{26}$$

which is a positive definite and radially unbounded function in the error vector space. Then we state

$$\begin{aligned}&\Delta Q_{t_n} = Q_{t_{n+1}} - Q_{t_n} = \\ &= \left(\left(I - hJ_{t_n}J_{\delta_{t_n}}^{-1}K_p\right)\breve{\boldsymbol{\eta}}_{t_n}+h\left(J_{t_n}\breve{\mathbf{v}}_{t_n}+J_{t_n}\delta\mathbf{v}_{t_n}+J_{t_n}J_{\delta_{t_n}}^{-1}\dot{\boldsymbol{\eta}}_{r_{t_n}}\right)+\right. \\ &\left.+\boldsymbol{\eta}_{r_{t_n}}-\boldsymbol{\eta}_{r_{t_{n+1}}}+\boldsymbol{\varepsilon}_{\eta_{n+1}}+\delta\boldsymbol{\eta}_{t_{n+1}}-\delta\boldsymbol{\eta}_{t_n}\right)^2-\breve{\boldsymbol{\eta}}_{t_n}^2+ \\ &+\left(\breve{\mathbf{v}}_{t_n}+J_{\delta_{t_n}}^{-1}\dot{\boldsymbol{\eta}}_{r_{t_n}}-J_{\delta_{t_{n+1}}}^{-1}\dot{\boldsymbol{\eta}}_{r_{t_{n+1}}}-J_{\delta_{t_n}}^{-1}K_p\breve{\boldsymbol{\eta}}_{t_n}+J_{\delta_{t_{n+1}}}^{-1}K_p\breve{\boldsymbol{\eta}}_{t_{n+1}}\right. \\ &\left.+hM^{-1}\left(\mathbf{p}_{\delta_{t_n}}+\boldsymbol{\tau}_n\right)+\delta\mathbf{v}_{t_{n+1}}-\delta\mathbf{v}_{t_n}+\boldsymbol{\varepsilon}_{v_{n+1}}\right)^2-\breve{\mathbf{v}}_{t_n}^2.\end{aligned} \tag{27}$$

The ideal path tracking demands that

$$\lim_{t_n\to\infty}\Delta Q_{t_n} = \lim_{t_n\to\infty}\left(Q_{t_{n+1}} - Q_{t_n}\right) = 0. \tag{28}$$

Bearing in mind the presence of disturbances and model uncertainties, the practical goal would be at least achieved that $\{\Delta Q_{t_n}\}$ remains bounded for $t_n \to \infty$.
In (Jordán & Bustamante, 2011) a flexible design of a completely adaptive digital controller was proposed. Therein all unknown system matrices (C_i, D_{q_i}, D_l, B_1 and B_2) that influence the stability of the control loop are adapted in the feedback control law with the unique exception of the inertia matrix M from which only a lower bound $\underline{M}$ is demanded. In that work a guideline to obtained an adequate value of that bound is indicated.
Here we will transcribe those results and continue afterwards the analysis to the aimed goal. First we can conveniently split the control thrust $\boldsymbol{\tau}_n$ into two terms as

$$\boldsymbol{\tau}_n = \boldsymbol{\tau}_{1_n} + \boldsymbol{\tau}_{2_n}, \tag{29}$$

where the first one is

$$\boldsymbol{\tau}_{1_n} = -K_v \overset{\smile}{\mathbf{v}}_{t_n} - \frac{1}{h}\underline{M}\left(J_{\delta_{t_n}}^{-1}\dot{\boldsymbol{\eta}}_{r_{t_n}} + J_{\delta_{t_n}}^{-1} K_p \overset{\smile}{\boldsymbol{\eta}}_{t_n} + \right. \\ \left. + J_{\delta_{t_{n+1}}}^{-1}\dot{\boldsymbol{\eta}}_{r_{t_{n+1}}} - J_{\delta_{t_{n+1}}}^{-1} K_p \overset{\smile}{\boldsymbol{\eta}}_{t_{n+1}} \right) - \mathbf{r}_{\delta_{t_n}}, \tag{30}$$

with $K_v = K_v^T \geq 0$ being another design matrix like K_p, but affecting the kinematic errors instead. The vector $\mathbf{r}_{\delta_{t_n}}$ is

$$\mathbf{r}_{\delta_{t_n}} = \sum_{i=1}^{6} U_i . \times C_{v_{i_{t_n}}} \mathbf{v}_{\delta_{t_n}} + U_7 \mathbf{v}_{\delta_{t_n}} + \\ + \sum_{i=1}^{6} U_{7+i} |v_{i_{t_n}}| \mathbf{v}_{\delta_{t_n}} + U_{14}\mathbf{g}_{1_{\delta_{t_n}}} + U_{15}\, \mathbf{g}_{2_{\delta_{t_n}}}, \tag{31}$$

where the matrices U_i in $\mathbf{r}_{\delta_{t_n}}$ will account for every unknown system matrix in $\mathbf{p}_{\delta_{t_n}}$ in order to build up the partial control action $\boldsymbol{\tau}_{1_n}$. Moreover, the U_i´s represent the matrices of the adaptive sampled-data controller which will be designed later. Besides, it is noticing that $\mathbf{r}_{\delta_{t_n}}$ and $\mathbf{p}_{\delta_{t_n}}$ contain noisy measures.

The definition of the second component $\boldsymbol{\tau}_{2_n}$ of $\boldsymbol{\tau}_n$ is more cumbersome than the first component $\boldsymbol{\tau}_{1_n}$.

Basically we attempt to modify ΔQ_{t_n} farther to confer the quadratic form particular properties of sign definiteness. To this end let us first put (30) into (27). Thus

$$\begin{aligned} \Delta Q_{t_n} &= Q_{t_{n+1}} - Q_{t_n} = \\ &= \left(\left(I - hJ_{t_n} J_{\delta_{t_n}}^{-1} K_p \right) \overset{\smile}{\boldsymbol{\eta}}_{t_n} + h \left(J_{t_n} \overset{\smile}{\mathbf{v}}_{t_n} + J_{t_n} \delta \mathbf{v}_{t_n} + J_{t_n} J_{\delta_{t_n}}^{-1} \dot{\boldsymbol{\eta}}_{r_{t_n}} \right) \right. \\ &+ \boldsymbol{\eta}_{r_{t_n}} - \boldsymbol{\eta}_{r_{t_{n+1}}} + \boldsymbol{\varepsilon}_{\eta_{n+1}} + \delta\boldsymbol{\eta}_{t_{n+1}} - \delta\boldsymbol{\eta}_{t_n} \Big)^2 - \overset{\smile}{\boldsymbol{\eta}}_{t_n}^2 + \\ &+ \left(\overset{\smile}{\mathbf{v}}_{t_n} + J_{\delta_{t_n}}^{-1}\dot{\boldsymbol{\eta}}_{r_{t_n}} - J_{\delta_{t_{n+1}}}^{-1}\dot{\boldsymbol{\eta}}_{r_{t_{n+1}}} - J_{\delta_{t_n}}^{-1} K_p \overset{\smile}{\boldsymbol{\eta}}_{t_n} + J_{\delta_{t_{n+1}}}^{-1} K_p \overset{\smile}{\boldsymbol{\eta}}_{t_{n+1}} - \right. \\ &\quad - hM^{-1} K_v \overset{\smile}{\mathbf{v}}_{t_n} - M^{-1}\underline{M}\left(J_{\delta_{t_n}}^{-1}\dot{\boldsymbol{\eta}}_{r_{t_n}} - J_{\delta_{t_n}}^{-1} K_p \overset{\smile}{\boldsymbol{\eta}}_{t_n} - J_{\delta_{t_{n+1}}}^{-1}\dot{\boldsymbol{\eta}}_{r_{t_{n+1}}} + J_{\delta_{t_{n+1}}}^{-1} K_p \overset{\smile}{\boldsymbol{\eta}}_{t_{n+1}} \right) \\ &\quad \left. + hM^{-1}\left(\mathbf{p}_{\delta_{t_n}} - \mathbf{r}_{\delta_{t_n}} \right) + hM^{-1}\boldsymbol{\tau}_{2_n} + \delta\mathbf{v}_{t_{n+1}} - \delta\mathbf{v}_{t_n} + \boldsymbol{\varepsilon}_{v_{n+1}} \right)^2 - \overset{\smile}{\mathbf{v}}_{t_n}^2, \end{aligned} \tag{32}$$

where the old definition of $J_{\delta_{t_n}}^{-1} = J^{-1}[\boldsymbol{\eta}_{t_n} + \delta\boldsymbol{\eta}_{t_n}]$ can be rewritten as

$$J_{\delta_{t_n}}^{-1} = J_{t_n}^{-1} + \Delta J_{t_n}^{-1}. \tag{33}$$

Now defining an motion vector function (combination of acceleration and velocity) in the form

$$\mathbf{s}_{t_n} = J_{\delta_{t_n}}^{-1}\dot{\boldsymbol{\eta}}_{r_{t_n}} - J_{\delta_{t_{n+1}}}^{-1}\dot{\boldsymbol{\eta}}_{r_{t_{n+1}}} - J_{\delta_{t_n}}^{-1} K_p \overset{\smile}{\boldsymbol{\eta}}_{t_n} + J_{\delta_{t_{n+1}}}^{-1} K_p \overset{\smile}{\boldsymbol{\eta}}_{t_{n+1}}, \tag{34}$$

the (32) turns into

$$\begin{aligned}\Delta Q_{t_n} &= Q_{t_{n+1}} - Q_{t_n} = \\ &= \Big((I - hK_p)\,\overset{\frown}{\boldsymbol{\eta}}_{t_n} - hJ_{t_n}\Delta J_{t_n}^{-1} K_p \overset{\frown}{\boldsymbol{\eta}}_{t_n} + h\left(J_{t_n}\overset{\frown}{\mathbf{v}}_{t_n} + \dot{\boldsymbol{\eta}}_{r_{t_n}}\right) + J_{t_n}\delta\mathbf{v}_{t_n} + J_{t_n}\Delta J_{t_n}^{-1}\dot{\boldsymbol{\eta}}_{r_{t_n}} \\ &+ \boldsymbol{\eta}_{r_{t_n}} - \boldsymbol{\eta}_{r_{t_{n+1}}} + \boldsymbol{\varepsilon}_{\eta_{n+1}} + \delta\boldsymbol{\eta}_{t_{n+1}} - \delta\boldsymbol{\eta}_{t_n}\Big)^2 - \overset{\frown}{\boldsymbol{\eta}}_{t_n}^2 + \\ &+ \Big(\left(I - hM^{-1}K_v\right)\overset{\frown}{\mathbf{v}}_{t_n} + \left(I - M^{-1}\underline{M}\right)\mathbf{s}_{t_n} - \\ &+ h\left(\mathbf{p}_{\delta_{t_n}} - M^{-1}\mathbf{r}_{\delta_{t_n}}\right) + hM^{-1}\boldsymbol{\tau}_{2_n} + \delta\mathbf{v}_{t_{n+1}} - \delta\mathbf{v}_{t_n} + \boldsymbol{\varepsilon}_{v_{n+1}}\Big)^2 - \overset{\frown}{\mathbf{v}}_{t_n}^2.\end{aligned} \tag{35}$$

From this expression one achieves

$$\begin{aligned}\Delta Q_{t_n} &= a(M^{-1}\boldsymbol{\tau}_{2_n})^2 + \mathbf{b}^T M^{-1}\boldsymbol{\tau}_{2_n} + c + \\ &+ \overset{\frown}{\boldsymbol{\eta}}_{t_n}^T \sqrt{a}K_p\left(\sqrt{a}K_p - 2I\right)\overset{\frown}{\boldsymbol{\eta}}_{t_n} + \\ &+ \overset{\frown}{\mathbf{v}}_{t_n}^T \sqrt{a}K_v^*\left(\sqrt{a}K_v^* - 2I\right)\overset{\frown}{\mathbf{v}}_{t_n} + \\ &+ f_{\Delta Q_{1_n}}[\boldsymbol{\varepsilon}_{\eta_{n+1}}, \boldsymbol{\varepsilon}_{v_{n+1}}, \delta\boldsymbol{\eta}_{t_{n+1}}, \delta\mathbf{v}_{t_{n+1}}],\end{aligned} \tag{36}$$

where K_v^* is an auxiliary matrix equal to $K_v^* = M^{-1}K_v$. The polynomial coefficients a, $\mathbf{b}$ and c are

$$a = h^2 \tag{37}$$

$$\begin{aligned}\mathbf{b} &= 2h(I - hK_v^*)\overset{\frown}{\mathbf{v}}_{t_n} + 2h\left(I - M^{-1}\underline{M}\right)\mathbf{s}_{t_n} + 2hM^{-1}\left(\mathbf{p}_{\delta_{t_n}} - \mathbf{r}_{\delta_{t_n}}\right) \\ &+ 2h\left(\delta\mathbf{v}_{t_{n+1}} - \delta\mathbf{v}_{t_n} + \boldsymbol{\varepsilon}_{v_{n+1}}\right)\end{aligned} \tag{38}$$

$$\begin{aligned}c &= h^2\left(J_{t_n}\overset{\frown}{\mathbf{v}}_{t_n} + \dot{\boldsymbol{\eta}}_{r_{t_n}}\right)^2 + \\ &+ 2h\left(J_{t_n}\overset{\frown}{\mathbf{v}}_{t_n} + \dot{\boldsymbol{\eta}}_{r_{t_n}}\right)^T\left(\boldsymbol{\eta}_{r_{t_n}} - \boldsymbol{\eta}_{r_{t_{n+1}}}\right) + \\ &+ \left(\boldsymbol{\eta}_{r_{t_n}} - \boldsymbol{\eta}_{r_{t_{n+1}}}\right)^T\left(\boldsymbol{\eta}_{r_{t_n}} - \boldsymbol{\eta}_{r_{t_{n+1}}}\right) + \\ &+ 2\left((I - hK_p)\,\overset{\frown}{\boldsymbol{\eta}}_{t_n}\right)^T\left(h(J_{t_n}\overset{\frown}{\mathbf{v}}_{t_n} + \dot{\boldsymbol{\eta}}_{r_{t_n}}) + \boldsymbol{\eta}_{r_{t_n}} - \boldsymbol{\eta}_{r_{t_{n+1}}}\right) + \\ &+ \left(I - M^{-1}\underline{M}\right)^2\mathbf{s}_{t_n}^2 + h^2M^{-1}\left(\mathbf{p}_{\delta_{t_n}} - \mathbf{r}_{\delta_{t_n}}\right)^2 + \left(\delta\mathbf{v}_{t_{n+1}} - \delta\mathbf{v}_{t_n} + \boldsymbol{\varepsilon}_{v_{n+1}}\right)^2 \\ &+ 2\left(\left(I - M^{-1}\underline{M}\right)\mathbf{s}_{t_n} + hM^{-1}\left(\mathbf{p}_{\delta_{t_n}} - \mathbf{r}_{\delta_{t_n}}\right)\right)^T\left(\delta\mathbf{v}_{t_{n+1}} - \delta\mathbf{v}_{t_n} + \boldsymbol{\varepsilon}_{v_{n+1}}\right)\end{aligned} \tag{39}$$

and $f_{\Delta Q_{1_n}}$ is a sign-undefined energy function of the model errors and measure disturbances defined as

$$\begin{aligned} & f_{\Delta Q_{1_n}}[\boldsymbol{\varepsilon}_{\eta_{n+1}},\boldsymbol{\varepsilon}_{v_{n+1}},\delta\boldsymbol{\eta}_{t_{n+1}},\delta\mathbf{v}_{t_{n+1}}] = \\ & \left(\boldsymbol{\varepsilon}_{\eta_{n+1}}+\delta\boldsymbol{\eta}_{t_{n+1}}-\delta\boldsymbol{\eta}_{t_n}-hJ_{t_n}\Delta J_{t_n}^{-1}K_p\overset{\frown}{\boldsymbol{\eta}}_{t_n}+J_{t_n}\delta\mathbf{v}_{t_n}+J_{t_n}\Delta J_{t_n}^{-1}\dot{\boldsymbol{\eta}}_{r_{t_n}}\right)^2 \\ & +2\left(\left(I-hK_p\right)\overset{\frown}{\boldsymbol{\eta}}_{t_n}+h\left(J_{t_n}\overset{\frown}{\mathbf{v}}_{t_n}+\dot{\boldsymbol{\eta}}_{r_{t_n}}\right)+\boldsymbol{\eta}_{r_{t_n}}-\boldsymbol{\eta}_{r_{t_{n+1}}}\right)^T\times \\ & \left(\boldsymbol{\varepsilon}_{\eta_{n+1}}+\delta\boldsymbol{\eta}_{t_{n+1}}-\delta\boldsymbol{\eta}_{t_n}-hJ_{t_n}\Delta J_{t_n}^{-1}K_p\overset{\frown}{\boldsymbol{\eta}}_{t_n}+J_{t_n}\delta\mathbf{v}_{t_n}+J_{t_n}\Delta J_{t_n}^{-1}\dot{\boldsymbol{\eta}}_{r_{t_n}}\right). \end{aligned} \tag{40}$$

Clearly, there are many variables involved like the system matrices, model errors and measure disturbances which are not known beforehand.
The idea now is to construct $\boldsymbol{\tau}_{2_n}$ so that the sum $a(M^{-1}\boldsymbol{\tau}_{2_n})^2+\mathbf{b}^TM^{-1}\boldsymbol{\tau}_{2_n}+c$ in (36) be null. As there are many variables in the sum which are unknown, we can construct an approximation of it with measurable variables. So, it results

$$\bar{a}\left(M^{-1}\boldsymbol{\tau}_{2_n}\right)^2+\overline{\mathbf{b}}_n^TM^{-1}\boldsymbol{\tau}_{2_n}+\bar{c}_n=0. \tag{41}$$

Now, the polynomial coefficients $\bar{a}$ $\overline{\mathbf{b}}_n$ and $\bar{c}_n$ are explained below. Here, there appear three error functions, namely $f_{\Delta Q_{1_n}}$, and the new functions $f_{\Delta Q_{2_n}}$ and $f_{U_{i_n}}$, all containing noisy and unknown variables which are described in the sequel.
The polynomial coefficients result

$$\bar{a} = a=h^2 \tag{42}$$

$$\overline{\mathbf{b}}_n = 2h(I-hK_v^*)\overset{\frown}{\mathbf{v}}_{t_n}+2h\underline{M}^{-1}(\overline{\mathbf{p}}_{\delta_{t_n}}-\mathbf{r}_{\delta_{t_n}}) \tag{43}$$

$$\begin{aligned} \bar{c}_n = {} & h^2\left(\left(J_{t_n}\overset{\frown}{\mathbf{v}}_{t_n}+\dot{\boldsymbol{\eta}}_{r_{t_n}}\right)^2+\left(\Delta J_{\delta t_n}\overset{\frown}{\mathbf{v}}_{t_n}\right)^2+2\left(J_{t_n}\overset{\frown}{\mathbf{v}}_{t_n}+\dot{\boldsymbol{\eta}}_{r_{t_n}}\right)^T\Delta J_{\delta t_n}\overset{\frown}{\mathbf{v}}_{t_n}\right)+ \\ & +2h\left(J_{t_n}\overset{\frown}{\mathbf{v}}_{t_n}+\dot{\boldsymbol{\eta}}_{r_{t_n}}\right)^T\left(\boldsymbol{\eta}_{r_{t_n}}-\boldsymbol{\eta}_{r_{t_{n+1}}}\right)+2h\left(\Delta J_{\delta t_n}\overset{\frown}{\mathbf{v}}_{t_n}\right)^T\left(\boldsymbol{\eta}_{r_{t_n}}-\boldsymbol{\eta}_{r_{t_{n+1}}}\right)+ \\ & +\left(\boldsymbol{\eta}_{r_{t_n}}-\boldsymbol{\eta}_{r_{t_{n+1}}}\right)^T\left(\boldsymbol{\eta}_{r_{t_n}}-\boldsymbol{\eta}_{r_{t_{n+1}}}\right)+ \\ & +2\left(\left(I-hK_p\right)\overset{\frown}{\boldsymbol{\eta}}_{t_n}\right)^T\left(h\left(J_{t_n}\overset{\frown}{\mathbf{v}}_{t_n}+\dot{\boldsymbol{\eta}}_{r_{t_n}}\right)+\boldsymbol{\eta}_{r_{t_n}}-\boldsymbol{\eta}_{r_{t_{n+1}}}\right)+2\left(\left(I-hK_p\right)\overset{\frown}{\boldsymbol{\eta}}_{t_n}\right)^T\left(h\Delta J_{\delta t_n}\overset{\frown}{\mathbf{v}}_{t_n}\right)+ \\ & +h^2\underline{M}^{-1}\left(\overline{\mathbf{p}}_{\delta_{t_n}}-\mathbf{r}_{\delta_{t_n}}\right)^2+2\left(h\underline{M}^{-1}(\overline{\mathbf{p}}_{\delta_{t_n}}-\mathbf{r}_{\delta_{t_n}})^T\right)(I-hK_v^*)\overset{\frown}{\mathbf{v}}_{t_n}, \end{aligned} \tag{44}$$

with $\overline{\mathbf{p}}_{\delta_{t_n}}$ being an estimation of $\mathbf{p}_{\delta_{t_n}}$ in (14) given by

$$\overline{\mathbf{p}}_{\delta_{t_n}}=\underline{M}\frac{\mathbf{v}_{t_n}-\mathbf{v}_{t_{n-1}}}{h}-\boldsymbol{\tau}_n. \tag{45}$$

The second component $\boldsymbol{\tau}_{2_n}$ of $\boldsymbol{\tau}_n$ was contained in the condition (41) like a root pair that enables ΔQ_{t_n} be the expression (47). It is

$$\boldsymbol{\tau}_{n_2}=\underline{M}\left(\frac{-\overline{\mathbf{b}}}{2\bar{a}}\pm\frac{1}{2\bar{a}}\sqrt{\frac{\overline{\mathbf{b}}^T\overline{\mathbf{b}}-4\bar{a}\bar{c}}{6}}\mathbf{1}\right), \tag{46}$$

with $\mathbf{1}$ being a vector with ones.
With the choice of (41) and (46) in ΔQ_{t_n} one gets finally

$$\begin{aligned}\Delta Q_{t_n} &= \overset{\frown}{\boldsymbol{\eta}}_{t_n}^T hK_p\left(hK_p-2I\right)\overset{\frown}{\boldsymbol{\eta}}_{t_n}+ \\ &+\overset{\frown}{\mathbf{v}}_{t_n}^T hK_v^*\left(hK_v^*-2I\right)\overset{\frown}{\mathbf{v}}_{t_n}+f_{\Delta Q_{1n}}[\boldsymbol{\varepsilon}_{\eta_{n+1}},\boldsymbol{\varepsilon}_{v_{n+1}},\delta\boldsymbol{\eta}_{t_{n+1}},\delta\mathbf{v}_{t_{n+1}}]+ \\ &+f_{\Delta Q_{2n}}[\boldsymbol{\varepsilon}_{\eta_{n+1}},\boldsymbol{\varepsilon}_{v_{n+1}},\delta\boldsymbol{\eta}_{t_{n+1}},\delta\mathbf{v}_{t_{n+1}}]+f_{U_{i_n}}[(U_i^*-U_i),M^{-1}\underline{M}].\end{aligned} \tag{47}$$

The matrices U_i^* that appear in $f_{U_{i_n}}$ take particular constant values of the adaptive controller matrices U_i´s. They take the values equal to the system matrices in (1)-(2) (Jordán and Bustamante, 2008), namely

$$U_i^* = C_i, \text{ with } i=1,...,6 \tag{48}$$

$$U_7^* = D_l \tag{49}$$

$$U_i^* = D_{q_i}, \text{ with } i=8,...,13 \tag{50}$$

$$U_{14}^* = B_1 \tag{51}$$

$$U_{15}^* = B_2\ . \tag{52}$$

Moreover, the error functions $f_{\Delta Q_{2_n}}$ and $f_{U_{i_n}}$ in (47) are respectively

$$\begin{aligned}f_{\Delta Q_{2_n}}[\boldsymbol{\varepsilon}_{\eta_{n+1}},\boldsymbol{\varepsilon}_{v_{n+1}},\delta\boldsymbol{\eta}_{t_{n+1}},\delta\mathbf{v}_{t_{n+1}}] &=2h\left(\delta\mathbf{v}_{t_{n+1}}-\delta\mathbf{v}_{t_n}+\boldsymbol{\varepsilon}_{v_{n+1}}\right)\times \\ \times M^{-1}\underline{M}\left(-\frac{\overline{\mathbf{b}}}{2\bar{a}}\pm\frac{1}{2\bar{a}}\sqrt{\frac{\overline{\mathbf{b}}^T\overline{\mathbf{b}}-4\bar{a}\bar{c}}{6}}\mathbf{1}\right)&-h^2\left(\Delta J_{\delta t_n}\overset{\frown}{\mathbf{v}}_{t_n}\right)^2- \\ -2h^2\left(\Delta J_{\delta t_n}\overset{\frown}{\mathbf{v}}_{t_n}\right)\left(\boldsymbol{\eta}_{r_{t_n}}-\boldsymbol{\eta}_{r_{t_{n+1}}}\right)&-2h^2\left(J_{t_n}\overset{\frown}{\mathbf{v}}_{t_n}+\dot{\boldsymbol{\eta}}_{r_{t_n}}\right)^T\Delta J_{\delta t_n}\overset{\frown}{\mathbf{v}}_{t_n}- \\ -2h\left(\left(I-hK_p\right)\overset{\frown}{\boldsymbol{\eta}}_{t_n}\right)^T\Delta J_{\delta t_n}\overset{\frown}{\mathbf{v}}_{t_n}&+\left(\delta\mathbf{v}_{t_{n+1}}-\delta\mathbf{v}_{t_n}+\boldsymbol{\varepsilon}_{v_{n+1}}\right)^2+ \\ +2\left(\left(I-M^{-1}\underline{M}\right)\mathbf{s}_{t_n}+hM^{-1}\left(\mathbf{p}_{\delta_{t_n}}-\mathbf{r}_{\delta_{t_n}}\right)\right)^T&\left(\delta\mathbf{v}_{t_{n+1}}-\delta\mathbf{v}_{t_n}+\boldsymbol{\varepsilon}_{v_{n+1}}\right),\end{aligned} \tag{53}$$

with $\Delta\mathbf{b}=\mathbf{b}-\overline{\mathbf{b}}$ from (38) and (43), and

$$f_{U_{i_n}}[(U_i^*-U_i),M^{-1}\underline{M}]= \tag{54}$$

$$\frac{\left(M^{-1}\underline{M}\,\overline{\mathbf{b}}\right)^T\left(M^{-1}\underline{M}\,\overline{\mathbf{b}}\right)}{4\bar{a}}+\frac{\mathbf{1}^T(M^{-1}\underline{M})^T(M^{-1}\underline{M})\mathbf{1}\left(\overline{\mathbf{b}}^T\,\overline{\mathbf{b}}\right)}{24\bar{a}}-\frac{\overline{\mathbf{b}}^T M^{-1}\underline{M}\,\overline{\mathbf{b}}}{2\bar{a}}\mp$$

$$\mp\overline{\mathbf{b}}^T\left(\left(M^{-1}\underline{M}\right)^T\left(M^{-1}\underline{M}\right)-M^{-1}\underline{M}\right)\frac{1}{2\bar{a}}\sqrt{\frac{\overline{\mathbf{b}}^T\,\overline{\mathbf{b}}-4\bar{a}\bar{c}}{6}}\mathbf{1}+$$

$$+2\left(h^2(M^{-1}-\underline{M}^{-1})K_v\overset{\frown}{\mathbf{v}}_{t_n}+h^2M^{-1}(\mathbf{p}_{\delta_{t_n}}-\mathbf{r}_{t_n})-h^2\underline{M}^{-1}(\bar{\mathbf{p}}_{t_n}-\mathbf{r}_{\delta_{t_n}})-\right.$$

$$\left.-h\left(I-M^{-1}\underline{M}\right)\mathbf{s}_{t_n}\right)^T M^{-1}\underline{M}\left(-\frac{\overline{\mathbf{b}}}{2\bar{a}}\pm\frac{1}{2\bar{a}}\sqrt{\frac{\overline{\mathbf{b}}^T\,\overline{\mathbf{b}}-4\bar{a}\bar{c}}{6}}\mathbf{1}\right)+h^2M^{-2}(\mathbf{p}_{\delta_{t_n}}-\mathbf{r}_{\delta_{t_n}})^2+$$

$$+\left(I-M^{-1}\underline{M}\right)^2\mathbf{s}_{t_n}^2+2h\left(M^{-1}(\mathbf{p}_{\delta_{t_n}}-\mathbf{r}_{\delta_{t_n}})\right)^T\left(I-M^{-1}\underline{M}\right)\mathbf{s}_{t_n}+$$

$$+2\left(h\left(M^{-1}(\mathbf{p}_{\delta_{t_n}}-\mathbf{r}_{\delta_{t_n}})\right)^T+\mathbf{s}_{t_n}^T\left(I-M^{-1}\underline{M}\right)^T\right)(I-hM^{-1}K_v)\overset{\frown}{\mathbf{v}}_{t_n}-$$

$$-h^2\underline{M}^{-2}\left(\overline{\mathbf{p}}_{\delta_{t_n}}-\mathbf{r}_{\delta_{t_n}}\right)^2-2\left(h\left(\underline{M}^{-1}\left(\overline{\mathbf{p}}_{\delta_{t_n}}-\mathbf{r}_{\delta_{t_n}}\right)\right)^T\right)(I-h\underline{M}^{-1}K_v)\overset{\frown}{\mathbf{v}}_{t_n}.$$

It is seeing from (40), (53) and (54), that the error functions go to lower bounds when $U_i=U_i^*$ (it is, when $\overline{\mathbf{p}}_{\delta_{t_n}}=\mathbf{r}_{\delta_{t_n}}$), $M^{-1}\underline{M}=I$ and $\delta\boldsymbol{\eta}_{t_{n+1}}=\delta\mathbf{v}_{t_{n+1}}=\mathbf{0}$. These bounds will ultimately depend on the model errors $\boldsymbol{\varepsilon}_{\eta_{n+1}}$ and $\boldsymbol{\varepsilon}_{v_{n+1}}$ only.

It is noticing from (46) that the roots may be either real or complex. Clearly when the roots are real, (41) is accomplished. If eventually complex roots appear, one can chose only the real part of the resulting complex roots, namely $\overline{\boldsymbol{\tau}}_{2_n}=\underline{M}\frac{-\overline{\mathbf{b}}_n}{2\bar{a}}$. The implications of that choice will be analyzed later in the section dedicated to the stability study.

Finally, the control action to be applied to the vehicle system is $\boldsymbol{\tau}_n=\boldsymbol{\tau}_{1_n}+\boldsymbol{\tau}_{2_n}$ with the two components given in (30) and (46), respectively.

4.2 Adaptive laws

According to a speed-gradient law (Fradkov et al., 1999), the adaptation of the system behavior occurs by the permanent actualization of the controller matrices U_i.

Let the following adaptive law be valid for $i=1,...,15$

$$U_{i_{n+1}}\overset{\Delta}{=}U_{i_n}-\Gamma_i\frac{\partial\Delta Q_{t_n}}{\partial U_i}, \tag{55}$$

with a gain matrix $\Gamma_i=\Gamma_i^T\geq 0$ and $\frac{\partial\Delta Q_{t_n}}{\partial U_{i_n}}$ being a gradient matrix for U_{i_n}.

First we can define an expression for the gradient matrix upon ΔQ_{t_n} in (47) but considering that M is known. This expression is referred to the ideal gradient matrix

$$\begin{aligned}\frac{\partial \Delta Q_{t_n}}{\partial U_i} = & -2h^2 M^{-T}\left(M^{-1}\boldsymbol{\tau}_{2_n}\right)\left(\frac{\partial \mathbf{r}_{\delta_{t_n}}}{\partial U_i}\right)^T - \\ & -2h^2 M^{-T} M^{-1}(\mathbf{p}_{\delta_{t_n}} - \mathbf{r}_{\delta_{t_n}})\left(\frac{\partial \mathbf{r}_{\delta_{t_n}}}{\partial U_i}\right)^T - \\ & -2hM^{-T}(I - hK_v^*)\widehat{\mathbf{v}}_{t_n}\left(\frac{\partial \mathbf{r}_{\delta_{t_n}}}{\partial U_i}\right)^T.\end{aligned} \tag{56}$$

Now, in order to be able to implement adaptive laws like (55) we have to replace the unknown M in (56) by its lower bound $\underline{M}$. In this way, we can generate implementable gradient matrices which will be denote by $\frac{\partial \overline{\Delta Q}_{t_n}}{\partial U_i}$ and is

$$\begin{aligned}\frac{\partial \overline{\Delta Q}_{t_n}}{\partial U_i} = & -2h^2 \underline{M}^{-T}\left(\underline{M}^{-1}\boldsymbol{\tau}_{2_n}\right)\left(\frac{\partial \mathbf{r}_{\delta_{t_n}}}{\partial U_i}\right)^T - \\ & -2h^2 \underline{M}^{-T}\underline{M}^{-1}(\overline{\mathbf{p}}_{\delta_{t_n}} - \mathbf{r}_{\delta_{t_n}})\left(\frac{\partial \mathbf{r}_{\delta_{t_n}}}{\partial U_i}\right)^T - \\ & -2h\underline{M}^{-T}(I - hK_v^*)\widehat{\mathbf{v}}_{t_n}\left(\frac{\partial \mathbf{r}_{\delta_{t_n}}}{\partial U_i}\right)^T,\end{aligned} \tag{57}$$

with the property

$$\frac{\partial \overline{\Delta Q}_{t_n}}{\partial U_i} = \frac{\partial \Delta Q_{t_n}}{\partial U_i} + \Delta_{U_{i_n}}, \tag{58}$$

where

$$\Delta_{U_{i_n}} = \delta_{M^{-2}} A_{i_n} + \delta_{M^{-1}} B_{i_n}, \tag{59}$$

and $\delta_{M^{-2}} = \left(\underline{M}^{-T}\underline{M}^{-1} - M^{-T}M^{-1}\right) \geq 0$ and $\delta_{M^{-1}} = \left(\underline{M}^{-1} - M^{-1}\right) \geq 0$. Here A_{i_n} and B_{i_n} are sampled state functions obtained from (56) after extracting of the common factors $\delta_{M^{-2}}$ and $\delta_{M^{-1}}$, respectively.

It is worth noticing that ΔQ_{t_n} and $\overline{\Delta Q}_{t_n}$, satisfy convexity properties in the space of elements of the U_i's.

Moreover, with (58) in mind we can conclude for any pair of values of U_i, say $U_i^{'}$ of $U_i^{''}$, it is valid

$$\Delta Q_{t_n}(U_i^{'}) - \Delta Q_{t_n}(U_i^{''}) \leq \frac{\partial \Delta Q_{t_n}(U_i^{''})}{\partial U_i}\left(U_i^{'} - U_i^{''}\right) \leq \tag{60}$$

$$\leq \frac{\partial \overline{\Delta Q}_{t_n}(U_i^{''})}{\partial U_i}\left(U_i^{'} - U_i^{''}\right). \tag{61}$$

This feature will be useful in the next analysis.

In summary, the practical laws which conform the digital adaptive controller are

$$U_{i_{n+1}} \triangleq U_{i_n} - \Gamma_i \frac{\partial \overline{\Delta Q}_{t_n}}{\partial U_i}. \tag{62}$$

Finally, it is seen from (57) that also here the noisy measures $\boldsymbol{\eta}_{\delta_{t_n}}$ and $\mathbf{v}_{\delta_{t_n}}$ will propagate into the adaptive laws $\frac{\partial \overline{\Delta Q}_{t_n}}{\partial U_i}$.

5. Stability analysis

In this section we prove stability, boundness of all control variables and convergence of the tracking errors in the case of path following for the case of 6 DOF´s involving references trajectories for position and kinematics.

5.1 Preliminaries

Let first the controller matrices U_i's to take the values U_i^*'s in (48)-(52). So, using these constant system matrices in (1),(4)-(6) and (14), a fixed controller can be designed.
For this particular controller we consider the resulting $\Delta Q_{t_n}^*$ from (47) accomplishing

$$\begin{aligned} \Delta Q_{t_n}^* = & \overset{\frown}{\boldsymbol{\eta}}_{t_n}^T hK_p \left(hK_p - 2I\right) \overset{\frown}{\boldsymbol{\eta}}_{t_n} + \\ & + \overset{\frown}{\mathbf{v}}_{t_n}^T hK_v^* \left(hK_v^* - 2I\right) \overset{\frown}{\mathbf{v}}_{t_n} + \\ & + f_{\Delta Q_n}^* [\boldsymbol{\varepsilon}_{\eta_{n+1}}, \boldsymbol{\varepsilon}_{v_{n+1}}, \delta\boldsymbol{\eta}_{t_n}, \delta\mathbf{v}_{t_n}, M^{-1}\underline{M}], \end{aligned} \tag{63}$$

where $f_{\Delta Q_n}^*$ is the sum of all errors obtained from (47) with (53) and (54). It fulfills with $\mathbf{p}_{\delta_{t_n}} = \mathbf{r}_{\delta_{t_n}}$

$$f_{\Delta Q_n}^* = f_{\Delta Q_{1_n}} + f_{\Delta Q_{2_n}}[\mathbf{p}_{\delta_{t_n}} = \mathbf{r}_{\delta_{t_n}}] + f_{U_{i_n}}[\mathbf{p}_{\delta_{t_n}} = \mathbf{r}_{\delta_{t_n}}]. \tag{64}$$

Later, a norm of $f_{\Delta Q_n}^*$ will be indicated.

Since $\left(\boldsymbol{\varepsilon}_{\eta_{n+1}} + \delta\boldsymbol{\eta}_{t_{n+1}} - \delta\boldsymbol{\eta}_{t_n}\right)$, $\left(\delta\mathbf{v}_{t_{n+1}} - \delta\mathbf{v}_{t_n} + \boldsymbol{\varepsilon}_{v_{n+1}}\right) \in l_\infty$ and $M^{-1}\underline{M} \in l_\infty$, then one concludes $f_{\Delta Q_n}^* \in l_\infty$ as well.
So, it is noticing that $\Delta Q_{t_n}^* < 0$, at least in an attraction domain equal to

$$\mathcal{B} = \left\{ \overset{\frown}{\boldsymbol{\eta}}_{t_n}, \overset{\frown}{\mathbf{v}}_{t_n} \in \mathcal{R}^6 \cap \mathcal{B}_0^* \right\}, \tag{65}$$

with $\mathcal{B}_0^*$ a residual set around zero

$$\mathcal{B}_0^* = \left\{ \overset{\frown}{\boldsymbol{\eta}}_{t_n}, \overset{\frown}{\mathbf{v}}_{t_n} \in \mathcal{R}^6 / \Delta Q_{t_n}^* - f_{\Delta Q_n}^* \leq 0 \right\} \tag{66}$$

and with the design matrices satisfying the conditions

$$\frac{2}{h} I > K_p \geq 0 \tag{67}$$

$$\frac{2}{h} I > K_v^* \geq 0, \tag{68}$$

which is equivalent to

$$\frac{2}{h}M \geq \frac{2}{h}\underline{M} > K_v \geq 0. \tag{69}$$

The residual set $\mathcal{B}_0^*$ depends not only on $\boldsymbol{\varepsilon}_{\eta_{n+1}}$ and $\boldsymbol{\varepsilon}_{v_{n+1}}$ and the measure noises $\delta\boldsymbol{\eta}_{t_n}$ and $\delta\mathbf{v}_{t_n}$, but also on $M^{-1}\underline{M}$. In consequence, $\mathcal{B}_0^*$ becomes the null point at the limit when $h \to 0$, $\delta\boldsymbol{\eta}_{t_n}$, $\delta\mathbf{v}_{t_n} \to 0$ and $\underline{M} = M$.

5.2 Stability proof

The problem of stability of the adaptive control system is addressed in the sequel. Let a Lyapunov function be

$$V_{t_n} = Q_{t_n} + \frac{1}{2}\sum_{i=1}^{15}\sum_{j=1}^{6}\left(\widetilde{\mathbf{u}}_j^T\right)_{i_{n+1}}\Gamma_i^{-1}\left(\widetilde{\mathbf{u}}_j\right)_{i_{n+1}} - \tag{70}$$

$$-\frac{1}{2}\sum_{i=1}^{15}\sum_{j=1}^{6}\left(\widetilde{\mathbf{u}}_j^T\right)_{i_n}\Gamma_i^{-1}\left(\widetilde{\mathbf{u}}_j\right)_{i_n},$$

with $\left(\widetilde{\mathbf{u}}_j\right)_{i_n} = \left(\mathbf{u}_j - \mathbf{u}_j^*\right)_{i_n}$, where $\mathbf{u}_j$ and $\mathbf{u}_j^*$ are vectors corresponding to the column j of the adaptive controller matrix U_i and its corresponding one U_i^* in the fixed controller, respectively. Then the differences $\Delta V_{t_n} = V_{t_{n+1}} - V_{t_n}$ can be bounded as follows

$$\Delta V_{t_n} = \Delta Q_{t_n} + \frac{1}{2}\sum_{i=1}^{15}\sum_{j=1}^{6}\left(\Delta\mathbf{u}_j^T\right)_{i_n}\Gamma_i^{-1}\left(\left(\widetilde{\mathbf{u}}_j\right)_{i_{n+1}} + \left(\widetilde{\mathbf{u}}_j\right)_{i_n}\right) \tag{71}$$

$$= \Delta Q_{t_n} + \sum_{i=1}^{15}\sum_{j=1}^{6}\left(\Delta\mathbf{u}_j^T\right)_{i_n}\Gamma_i^{-1}\left(\widetilde{\mathbf{u}}_j\right)_{i_n} - \frac{1}{2}\sum_{i=1}^{15}\sum_{j=1}^{6}\left(\Delta\mathbf{u}_j^T\right)_{i_n}\Gamma_i^{-1}\left(\Delta\mathbf{u}_j\right)_{i_n}$$

$$\leq \Delta Q_{t_n} - \sum_{i=1}^{15}\sum_{j=1}^{6}\left(\frac{\partial\Delta Q_{t_n}}{\partial\mathbf{u}_j}\right)^T\left(\widetilde{\mathbf{u}}_j\right)_{i_n}$$

$$\leq \Delta Q_{t_n} - \sum_{i=1}^{15}\sum_{j=1}^{6}\left(\frac{\partial\overline{\Delta Q}_{t_n}}{\partial\mathbf{u}_j}\right)^T\left(\widetilde{\mathbf{u}}_j\right)_{i_n}$$

$$\leq \Delta Q_{t_n}^* < 0 \text{ in } \mathcal{B}\cap\mathcal{B}_0^*,$$

with $\left(\Delta\mathbf{u}_j\right)_{i_n}$ a column vector of $\left(U_{i_{n+1}} - U_{i_n}\right)$.

The column vector $\left(\Delta\mathbf{u}_j\right)_{i_n}$ at the first inequality was replaced by the column vector $-\Gamma_i\left(\frac{\partial\Delta Q_{t_n}}{\partial\mathbf{u}_j}\right)$ and then by $-\Gamma_i\left(\frac{\partial\overline{\Delta Q}_{t_n}}{\partial\mathbf{u}_j}\right)$ in the right member according to (58) and (60)-(61). So in the second and third inequality, the convexity property of ΔQ_{t_n} in (60) was applied for any pair $\left(U' = U_{i_n}, U'' = U_i^*\right)$.

This analysis has proved convergence of the error paths when real square roots exist from $\sqrt{\overline{\mathbf{b}}_n^T\overline{\mathbf{b}}_n - 4\bar{a}\bar{c}_n}$ of (46).

If on the contrary $4\bar{a}\bar{c}_n > \overline{\mathbf{b}}_n^T\overline{\mathbf{b}}_n$ occurs at some time t_n, one chooses the real part of the complex roots in (46). So a suboptimal control action is employed instead, In this case, it is valid

$$\boldsymbol{\tau}_{2_n} = \frac{-1}{2\bar{a}}\underline{M}^{-1}\overline{\mathbf{b}}_n = \frac{-\underline{M}^{-1}}{h}(I - hK_v^*)\overset{\frown}{\mathbf{v}}_{t_n}. \tag{72}$$

So it yields a new functional $\Delta Q_{t_n}^{**}$ in

$$\Delta V_{t_n} \leq \Delta Q_{t_n}^{**} = \Delta Q_{t_n}^{*} + \bar{c}_n - \frac{1}{4h^2}\overline{\mathbf{b}}_n^T\overline{\mathbf{b}}_n < 0 \text{ in } \mathcal{B} \cap \mathcal{B}_0^{**}, \tag{73}$$

where $\Delta Q_{t_n}^{*}$ is (63) with a real root of (46) and $\mathcal{B}_0^{**}$ is a new residual set. It is worth noticing that the positive quantity $\left(\bar{c}_n - \frac{1}{4h^2}\overline{\mathbf{b}}_n^T\overline{\mathbf{b}}_n\right)$ can be reduced by choosing h small. Nevertheless, $\mathcal{B}_0^{**}$ results larger than $\mathcal{B}_0^{*}$ in (71), since its dimension depends not only on $\boldsymbol{\varepsilon}_{\eta_{n+1}}$ and $\boldsymbol{\varepsilon}_{v_{n+1}}$ but also on the magnitude of $\left(\bar{c}_n - \frac{1}{4h^2}\overline{\mathbf{b}}_n^T\overline{\mathbf{b}}_n\right)$.
This closes the stability and convergence proof.

5.3 Variable boundness

With respect to the boundness of the adaptive matrices U_i´s it is seen from (57) that the gradients are bounded. Also the third term is more dominant than the remainder ones for h small ($h << 1$), and so, the kinematic error $\overset{\frown}{\mathbf{v}}_{t_n}$ influences the intensity and sign of $\partial\overline{\Delta Q}_{t_n}/\partial U_i$ more significantly than the others. From (62) one concludes than the increasing of $|U_i|$ may not be avoided long term, however some robust modification techniques like a projection zone can be employed to achieve boundness. This is not developed here. The author can consult for instance (Ioannou and Sun, 1995).

5.4 Incidence of model errors and noisy measures

It is seen in (66) that the residual set $\mathcal{B}_0^{*}$ is conformed by the perturbation error function $f_{\Delta Q_n}^{*}$. In this section some guidelines can be given for a proper selection of the design parameters in order to diminish the incidence of model errors and noisy measures. This concerns the design matrices K_p and K_v as well as operation parameters like the cruise vehicle velocity and the control action self.
To this end, let the sign-undefined term $f_{\Delta Q_n}^{*}$ be upper bounded by

$$\begin{aligned}
\left|f_{\Delta Q_n}^{*}\right| \leq\ & |\mathbf{f}_1|\,|\boldsymbol{\varepsilon}_{\eta_{n+1}} + \delta\boldsymbol{\eta}_{t_{n+1}} - \delta\boldsymbol{\eta}_{t_n}| + |\mathbf{f}_1|\,|J_{t_n}|\left|\Delta J_{t_n}^{-1}K_p\overset{\frown}{\boldsymbol{\eta}}_{t_n} + \Delta J_{t_n}^{-1}\dot{\boldsymbol{\eta}}_{r_{t_n}}\right| + |\mathbf{f}_1|\,|J_{t_n}|\,|\delta\mathbf{v}_{t_n}| + \\
& + |\mathbf{f}_2|\left|\Delta J_{\delta t_n}\overset{\frown}{\mathbf{v}}_{t_n}\right| + |\mathbf{f}_3|\,|\boldsymbol{\varepsilon}_{v_{n+1}} + \delta\mathbf{v}_{t_{n+1}} - \delta\mathbf{v}_{t_n}| + \\
& 2h\left|M^{-1}\overline{\boldsymbol{\tau}}_{2_n}\right|\,|\boldsymbol{\varepsilon}_{v_{n+1}} + \delta\mathbf{v}_{t_{n+1}} - \delta\mathbf{v}_{t_n}| + h^2\left|\Delta J_{\delta t_n}\overset{\frown}{\mathbf{v}}_{t_n}\right|^2 \\
& + \left|\boldsymbol{\varepsilon}_{\eta_{n+1}} + \delta\boldsymbol{\eta}_{t_{n+1}} - \delta\boldsymbol{\eta}_{t_n} - hJ_{t_n}\Delta J_{t_n}^{-1}K_p\overset{\frown}{\boldsymbol{\eta}}_{t_n} + J_{t_n}\delta\mathbf{v}_{t_n} + J_{t_n}\Delta J_{t_n}^{-1}\dot{\boldsymbol{\eta}}_{r_{t_n}}\right|^2 \\
& + |\boldsymbol{\varepsilon}_{v_{n+1}} + \delta\mathbf{v}_{t_{n+1}} - \delta\mathbf{v}_{t_n}|^2 + \\
& + |f_4|\left|I - M^{-1}\underline{M}\right|,
\end{aligned} \tag{74}$$

where $\mathbf{f}_1$,$\mathbf{f}_2$ and $\mathbf{f}_3$ are bounded vector functions

$$\mathbf{f}_1^T = 2\left((I - hK_p)\,\widehat{\boldsymbol{\eta}}_{t_n} + h\left(J_{t_n}\widehat{\mathbf{v}}_{t_n} + \dot{\boldsymbol{\eta}}_{r_{t_n}} \right) + \boldsymbol{\eta}_{r_{t_n}} - \boldsymbol{\eta}_{r_{t_{n+1}}} \right)^T \tag{75}$$

$$\mathbf{f}_2^T = -2h\left(h\left(\boldsymbol{\eta}_{r_{t_n}} - \boldsymbol{\eta}_{r_{t_{n+1}}} \right) + h\left(J_{t_n}\widehat{\mathbf{v}}_{t_n} + \dot{\boldsymbol{\eta}}_{r_{t_n}} \right) + (I - hK_p)\,\widehat{\boldsymbol{\eta}}_{t_n} \right)^T \tag{76}$$

$$\mathbf{f}_3^T = \left(\left(I - M^{-1}\underline{M} \right)\mathbf{s}_{t_n} \right)^T, \tag{77}$$

and f_4 is also a bounded scalar function which can be identified from (54) with $\mathbf{p}_{\delta_{t_n}} = \mathbf{r}_{\delta_{t_n}}$ as

$$f_{U_i}[\mathbf{p}_{\delta_{t_n}} = \mathbf{r}_{\delta_{t_n}}] = \tag{78}$$

$$\frac{\left(M^{-1}\underline{M}\,\overline{\mathbf{b}} \right)^T \left(M^{-1}\underline{M}\,\overline{\mathbf{b}} \right)}{4\bar{a}} + \frac{\mathbf{1}^T (M^{-1}\underline{M})^T (M^{-1}\underline{M})\mathbf{1}\left(\overline{\mathbf{b}}^T\,\overline{\mathbf{b}} \right)}{24\bar{a}} - \frac{\overline{\mathbf{b}}^T M^{-1}\underline{M}\,\overline{\mathbf{b}}}{2\bar{a}} \mp$$

$$\mp \overline{\mathbf{b}}^T \left(\left(M^{-1}\underline{M} \right)^T \left(M^{-1}\underline{M} \right) - M^{-1}\underline{M} \right) \frac{1}{2\bar{a}} \sqrt{\frac{\overline{\mathbf{b}}^T\,\overline{\mathbf{b}} - 4\bar{a}\bar{c}}{6}}\,\mathbf{1} +$$

$$+2\left(h^2 (M^{-1} - \underline{M}^{-1}) K_v \widehat{\mathbf{v}}_{t_n} - h\left(I - M^{-1}\underline{M} \right)\mathbf{s}_{t_n} \right)^T M^{-1}\overline{\boldsymbol{\tau}}_{2_n} +$$

$$+ \left(I - M^{-1}\underline{M} \right)^2 \mathbf{s}_{t_n}^2 + 2\,\mathbf{s}_{t_n}^T \left(I - M^{-1}\underline{M} \right)^T (I - hM^{-1}K_v)\widehat{\mathbf{v}}_{t_n},$$

where the norm $\left| I - M^{-1}\underline{M} \right|$ is implicitly contained herein.
Clearly, if $h \to 0$, $\delta\boldsymbol{\eta}_{t_n}$, $\delta\mathbf{v}_{t_n} \to 0$ and $\underline{M} = M$, then $f^*_{\Delta Q_n}$ tends to zero conjointly.
At the first glance in (64) and (53), one notices that the inertia matrix M appears in $\mathbf{f}_3$. So, it is valid

$$\frac{|\mathbf{f}_3|}{|\mathbf{s}_{t_n}|} \leq \left(1 - \lambda_{\min}\left[M^{-1}\underline{M} \right] \right) || \tag{79}$$

which does reveal that the influence of M on $\mathbf{f}_3$ is reduced whatever $\underline{M}$ be a good estimate of M, it is when $\lambda_{\min}\left[M^{-1}\underline{M} \right]$ be close to one. Besides, no dependence of the sampling time h on $\mathbf{f}_3$ is observed any longer in the tightest bound in (79).
Since the body inertia matrix M_b is plausible to be good estimated, we can choose $\underline{M} = M_b$. So it is valid

$$\frac{|\mathbf{f}_3|}{|\mathbf{s}_{t_n}|} \leq 1 - \left| (M_b + M_a)^{-1} \right| |M_b|\,. \tag{80}$$

Particularly, AUVs are designed with hydrodynamically slender profiles, they have commonly much more smaller values of M_a than in the case of ROVs. In this sense, it is expected that the uncertainty M_a affect more the steady-state performance in ROVs than in AUVs.
The same analysis can be carried out for $\mathbf{f}_1$in (74). In particular, a choice of K_p in $\mathbf{f}_1$ that is as close as possible to the value I/h (see (67)), will reduce partially $|\mathbf{f}_1|$. Analogously, the same result for K_p could be obtained from $\mathbf{f}_2$.

On the other side, one sees that small differences of $\left(\boldsymbol{\eta}_{r_{t_n}} - \boldsymbol{\eta}_{r_{t_{n+1}}}\right)$ or equivalently small values of $\dot{\boldsymbol{\eta}}_{r_{t_n}}$ have the influence of decreasing $|\mathbf{f}_1|$ as well. Since the quantity $\dot{\boldsymbol{\eta}}_{r_{t_n}} - \frac{\boldsymbol{\eta}_{r_{t_{n+1}}} - \boldsymbol{\eta}_{r_{t_n}}}{h}$ assumes small values for h small, then large cruise velocities do not affect the performance if the sampling time is chosen relatively small.

Besides, the term $hJ_{t_n}\widehat{\mathbf{v}}_{t_n}$ in $\mathbf{f}_1$ leads to the same conclusion about the effect of h. However, it is interesting to stress the fact that appears in vehicle rotations which may rise the norm of $J_{t_n}[\varphi, \theta, \psi]$ considerably when the pitch angle goes above about 30° (Jordán & Bustamante, 2011).

The scalar function f_4, whose bound is implicitly included in (78) gets small when particularly the vector $\overline{\mathbf{b}}$ is small (this means also $\overline{\boldsymbol{\tau}}_{n_2}$ small), and the motion vector function $\mathbf{s}_{t_n}$ is also rather moderate.

Finally, there is the term $2h\overline{\boldsymbol{\tau}}_{2_n}$ in (74) that also contributes to increase $f_{\Delta Q_{2_n}}$ particularly when saturation values of the thrusters are achieved. Since $\overline{\boldsymbol{\tau}}_{2_n}$ is fixed by the controller, the only countermeasure to be applied lays in the fact that the controller always choose the lower $\overline{\boldsymbol{\tau}}_{2_n}$ of the two possible roots in (46). So, the perturbation energy $f_{\Delta Q_{2_n}}$ is reduced as far as possible by the controller.

From (63) one can draw out that the choice $K_v = \frac{1}{h}M_b$ in the negative definite terms is much more appropriate to increase the negativeness of $\Delta Q^*_{t_n}$. Equally the choice of K_p in the same manner helps the trajectories to get the residual set more rapid.

Besides, the model errors and noisy measures $(\boldsymbol{\varepsilon}_{v_{n+1}} + \delta\mathbf{v}_{t_{n+1}} - \delta\mathbf{v}_{t_{n+1}})$ and $\left(\boldsymbol{\varepsilon}_{\eta_{n+1}} + \delta\boldsymbol{\eta}_{t_{n+1}} - \delta\mathbf{v}_{t_{n+1}}\right)$ enter linearly and quadratically in the energy equation (74). As they are usually small, only the linear terms are magnified/attenuated by $\mathbf{f}_1$, $\mathbf{f}_2$, $\mathbf{f}_3$ and $\overline{\boldsymbol{\tau}}_{2_n}$, while f_4 impacts nonlinearly in $\overline{\boldsymbol{\tau}}_{n_2}$ and $\mathbf{s}_{t_n}$ as seen in (54).

5.5 Instability for large sampling time

Broadly speaking, the influence of the analyzed parameters will play a role in the instability when (on the chosen h is something large, even smaller than one, because the quadratic terms rise significantly to turn to be dominant in the error function $f^*_{\Delta Q_n}$.

The study of this phenomenon is rather complex but it generally involves the function $\Delta Q^*_{t_n}$ in (63) and $f^*_{\Delta Q_n}$ in (64).

For instante, when

$$f^*_{\Delta Q_n} > \widehat{\boldsymbol{\eta}}^T_{t_n} hK_p \left(hK_p - 2I\right) \widehat{\boldsymbol{\eta}}_{t_n} + \widehat{\mathbf{v}}^T_{t_n} hK^*_v \left(hK^*_v - 2I\right) \widehat{\mathbf{v}}_{t_n}, \tag{81}$$

the path trajectories may not be bounded into a residual set because the domain for the initial conditions in this situation is partially repulsive. So, depending on the particular initial conditions and for $h >> 0$ the adaptive control system may turn unstable.

In conclusion, when comparing two digital controllers, the sensitivity of the stability to h is fundamental to draw out robust properties and finally to range them.

6. Adaptive control algorithm

The adaptive control algorithm can be summarized as follows.

Preliminaries:

1) Estimate a lower bound $\underline{M}$, for instance $\underline{M} = M_b$ (Jordán & Bustamante, 2011),

2) Select a sampling time h as smaller as possible
3) Choose design gain matrices K_p and K_v according to (68)-(69), and simultaneously in order to reduce $f^*_{\Delta Q_n}$ and $\Delta Q^*_{t_n}$ (see related commentary in previous section),
4) Define the adaptive gain matrices Γ_i (usually $\Gamma_i = \alpha_i I$ with $\alpha_i > 0$),
5) Stipulate the desired sampled-data path references for the geometric and kinematic trajectories in 6 DOF´s: $\boldsymbol{\eta}_{r_{t_n}}$ and $\mathbf{v}_{r_{t_n}}$, respectively (see related commentary in previous section).
Continuously at each sample point:
6) Calculate the control thrust $\boldsymbol{\tau}_n$ with components $\boldsymbol{\tau}_{1_n}$ in (30) and $\boldsymbol{\tau}_{2_n}$ (46) (or (72)), respectively,
7) Calculate the adaptive controller matrices (56) with the lower bound $\underline{M}$ instead of M.
Long-term tuning:
7) Redefine K_p, K_v and h in order to achieve optimal tracking performance.

7. Case study

7.1 Setup

With the end of illustrating the features of our control system approach, we simulate a path-tracking problem in 6 DOF´s for an underwater vehicle in a planar motion with some sporadic immersions to the floor.
A continuous-time model of a fully-maneuverable underwater vehicle is employed for the numerical simulations. Details of this dynamics are given in (Jordán & Bustamante, 2009c). The propulsion system is composed by 8 thrusters, distributed in 4 vertical and 4 horizontal.
The simulated reference path $\boldsymbol{\eta}_r$ and the navigation path $\boldsymbol{\eta}$ are reproduced together by means of a visualization program (see a photogram in Fig. 2). The units for the path run away are in meters.
Basically the vehicle turns around a planar path. At a certain coordinate A it leaves the plane and submerses to the point A' for picking up a sample (of weight 10 (Kgf)) on the sea floor and returns back to A with a typical maneuver (backward movement and rotation). Then it continues on the planar trajectory till the coordinate B in where it submerses again to the point B' in order to place an equipment on the floor (of weight 20 (Kgf)) before to retreat and turn back to B and to complete finally the cycle. The vehicle weight is about 60 (kgf).
Additionally to the geometric path, the rate function $\mathbf{v}_r(t) = J^{-1}(\boldsymbol{\eta}_r)\dot{\boldsymbol{\eta}}_r(t)$ along it, is also specified, with short periods of rest at points A' and B' before beginning and after ending the maneuvers on the bottom.
At the start point of the mission (represented by O in Fig. 2), it is assumed for the adaptive control there is no information available about the vehicle dynamics matrices. Moreover, the maneuvers at stretches A-A' and B-B' imply considerable changes of moments acting on the vehicle in both a positive and negative quantities.
The reference velocity is programmed to be constant equal to 0.25(m/s) for the advance and as well as for the descent/ascent along the path. This rate will be referred to as the cruise velocity.
By the simulations, the adaptive control algorithm summarized in the previous section, is implemented. It is coupled with the ODE (1)-(2) for the vehicle dynamics, whose solution is numerically calculated in continuous time using Runge-Kutta approximators (the so-called *ODE45*). The computed control action is connected to a zero-order sample&hold previously to excite the vehicle.

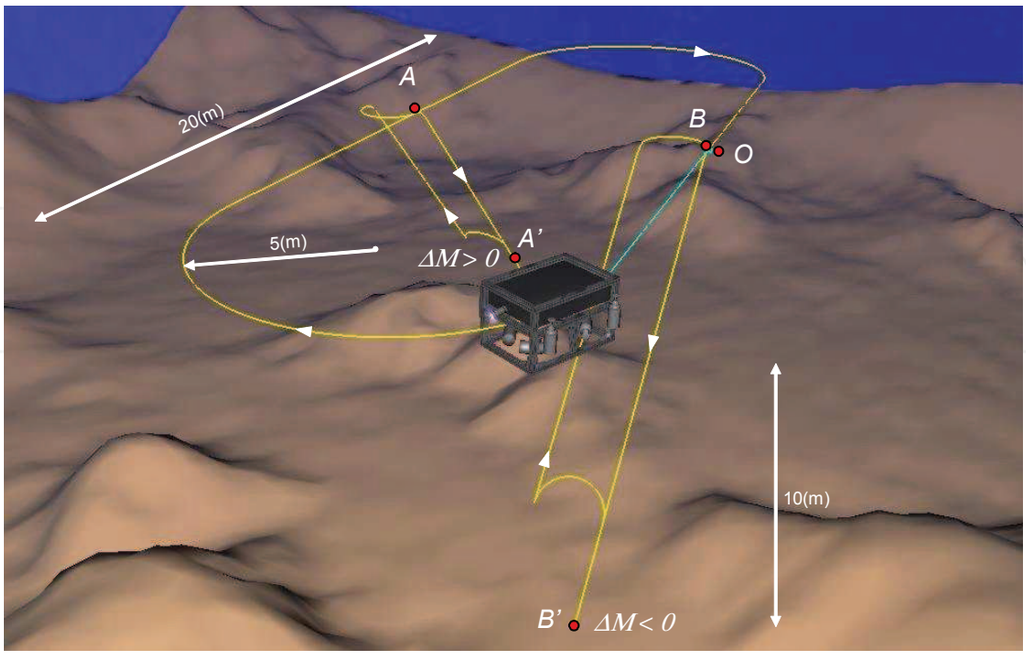

Fig. 2. Path tracking with grab sampling at coordinate A', and with placing of an equipment on the seafloor at coordinate B'

7.2 Design parameters

The most important *a-priori* information for the adaptive controller design is the ODE-structure in (1)-(2) but not its dynamics matrices, with the exception of the lower bound for the inertia matrix M. This takes the form

$$M = M_b + M_a \tag{82}$$

with the components: the body matrix M_b and the additive matrix M_a given by

$$M_b = M_{b_n} + \delta(t - t_{A'})\, M_{b\Delta^+} - \delta(t - t_{B'})\, M_{b\Delta^-} \tag{83}$$

$$M_a = M_{a_n} + \delta(t - t_{A'})\, M_{a\Delta^+} - \delta(t - t_{B'})\, M_{a\Delta^-}, \tag{84}$$

where M_{b_n} and M_{a_n} are nominal values of M_b and M_a at the start point O, and $M_{b\Delta^-}, M_{b\Delta^+}, M_{a\Delta+}$ and $M_{a\Delta-}$ are positive and negative variations at instants $t_{A'}$ and $t_{B'}$ on the points A' and B' of Fig. 2. Here $\delta(t - t_i)$ represents the Dirac function.

For our application M_{b_n} is determinable beforehand experimentally and it is set as the lower bound $\underline{M}$ for the control and adaptive laws. In the simulated scenario, $M_{b\Delta^-}$ is assumed known because it is about of an equipment deposited on the seafloor. In the case of $M_{b\Delta^+}$, $M_{a\Delta^+}$ and even $M_{a\Delta^-}$, we depart from unknown values.

The property of $M_a \geq 0$ is not affected by the sign of $M_{a\Delta^+}$ and $M_{a\Delta^-}$, which may be positive and negative as well. For that reason, a valid lower bound is chosen as $\underline{M} = M_{b_n} - M_{b\Delta^-}$.

Taking into account the simulation setup for the weight changes (the weight picked up from the seafloor at $t_{A'}$ and the second weight deposited on the seafloor at $t_{B'}$), the lower bound for $\underline{M}$ is

$$\underline{M} = \mathrm{diag}(60, 60, 60, 5, 10, 10), \tag{85}$$

and the mass variations are

$$M_{b\Delta^+} = \text{diag}(10, 10, 10, 0.6250, 4.2250, 3.6) \tag{86}$$
$$M_{b\Delta^-} = \text{diag}(20, 20, 20, 1.25, 1.25, 0) \tag{87}$$
$$M_{a\Delta+} = \text{diag}(6.3, 15.4, 0.115, 0.115, 0.261, 0.276) \tag{88}$$
$$M_{a\Delta^-} = \text{diag}(12.6, 30.8, 0.23, 0.23, 0.521, 0.551). \tag{89}$$

The design gain matrices for the controller are

$$\begin{aligned} K_p &= \text{diag}\,(5, 5, 5, 5, 5, 5) \\ K_v &= \text{diag}\,(300, 300, 300, 25, 50, 50) \end{aligned} \tag{90}$$

and the adaptive gain matrices about

$$\Gamma_i = I. \tag{91}$$

Finally we have proposed a sampling time $h = 0.2$(s).
All quantities are expressed in the SI Units.

7.3 Control performance

Here the acquired performance by the autonomously guided vehicle under the described simulated setup will be evaluated. First, in Fig. 3, the path error evolution corresponding to every mode with their respective rates is shown for the different transient phases, namely: the controller autotuning at the initial phase (to the left), the sampling phase on the sea bottom at A' (in the middle), and the release of an equipment on the floor at B' (to the right).
The largest path errors had occurred during the initial phase because the amount of information for the control adaptation was null. Here, the longest transient took about 5(s) which is considered outstanding in comparison to the commonly slow open loop behavior. Later, after the mass changes, the path errors behaved much more moderate and were insignificant in magnitude (only a few centimeters or a few hundredths of a radian according to translation/rotation). Among them, the errors in the surge, sway and pitch modes (x, z and θ) resulted more perturbed than the remainder ones because they were more excited from the main motion provided by the stipulated mission. In all evolutions the adaptations occurred quick and smoothly.
The same scenario of control performance can be observed in Fig. 4 from the side of the velocity path errors for every mode of motion. Qualitatively, all kinematic path errors were attenuated rapid and smoothly in the autotuning phase as well as during the mass-change periods. The magnitude of these errors is also related to the rapid changes of the reference $\mathbf{v}_{ref}$ in the programmed maneuvers.
In the Fig. 5, the time evolution of the actuator thrust for two arbitrarily selected thrusters (one horizontal and one vertical) is shown. Analogously as previous results, the forces are compared within the three periods of transients. One observes that the intervention of the controller after a sudden change of mass occurred immediately. Also the transients of these interventions up to the practical steady state were relatively short.
Fig. 6 illustrates the time evolution of some controller matrices U_i. To this end, we had chosen the induced norm of U_8 which is partially related to the adaptation of the linear damping.
One sees that the norm of U_8 evolved with significative changes. In contrast to analog adaptive controllers of the speed-gradient class, here the U_i's do not tend asymptotically to

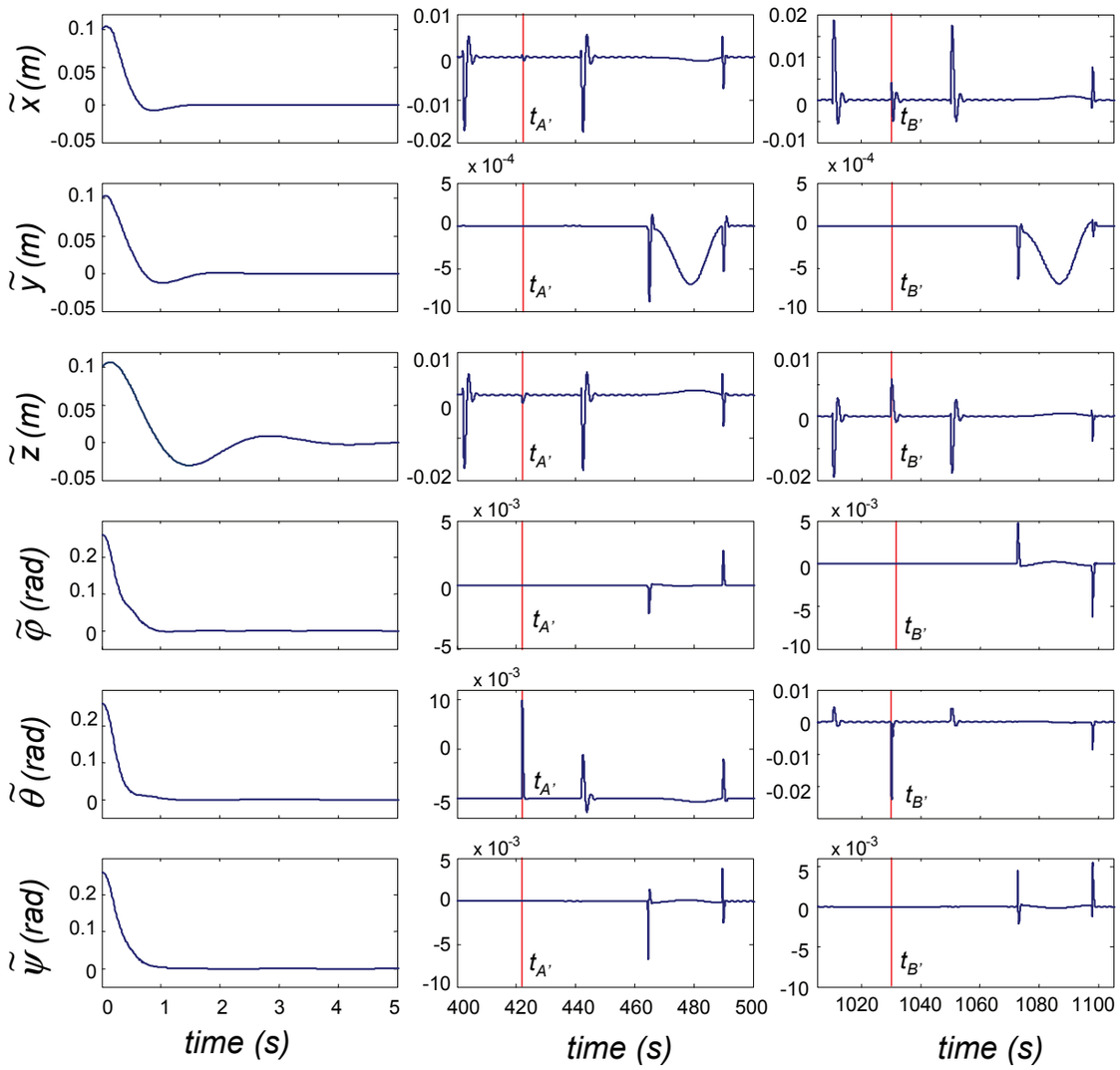

Fig. 3. Position path errors during transients in three different periods (from left to right column: autotuning, adaptation by weight pick up and adaptation by weight deposit)

constant matrices because of the difference between $\underline{M}^{-1}$ and M^{-1} in (58)-(59) (cf. Jordán & Bustamante, 2009c).

8. Conclusions

In this paper a novel design of adaptive control systems was presented. This is based on speed-gradient techniques which are widespread in the form of continuous-time designs in the literature. Here, we had focused their counterparts namely sampled-data adaptive controllers.

The work was framed into the path tracking control problem for the guidance of vehicles in many degrees of freedom. Particularly, the most complex dynamics of this class

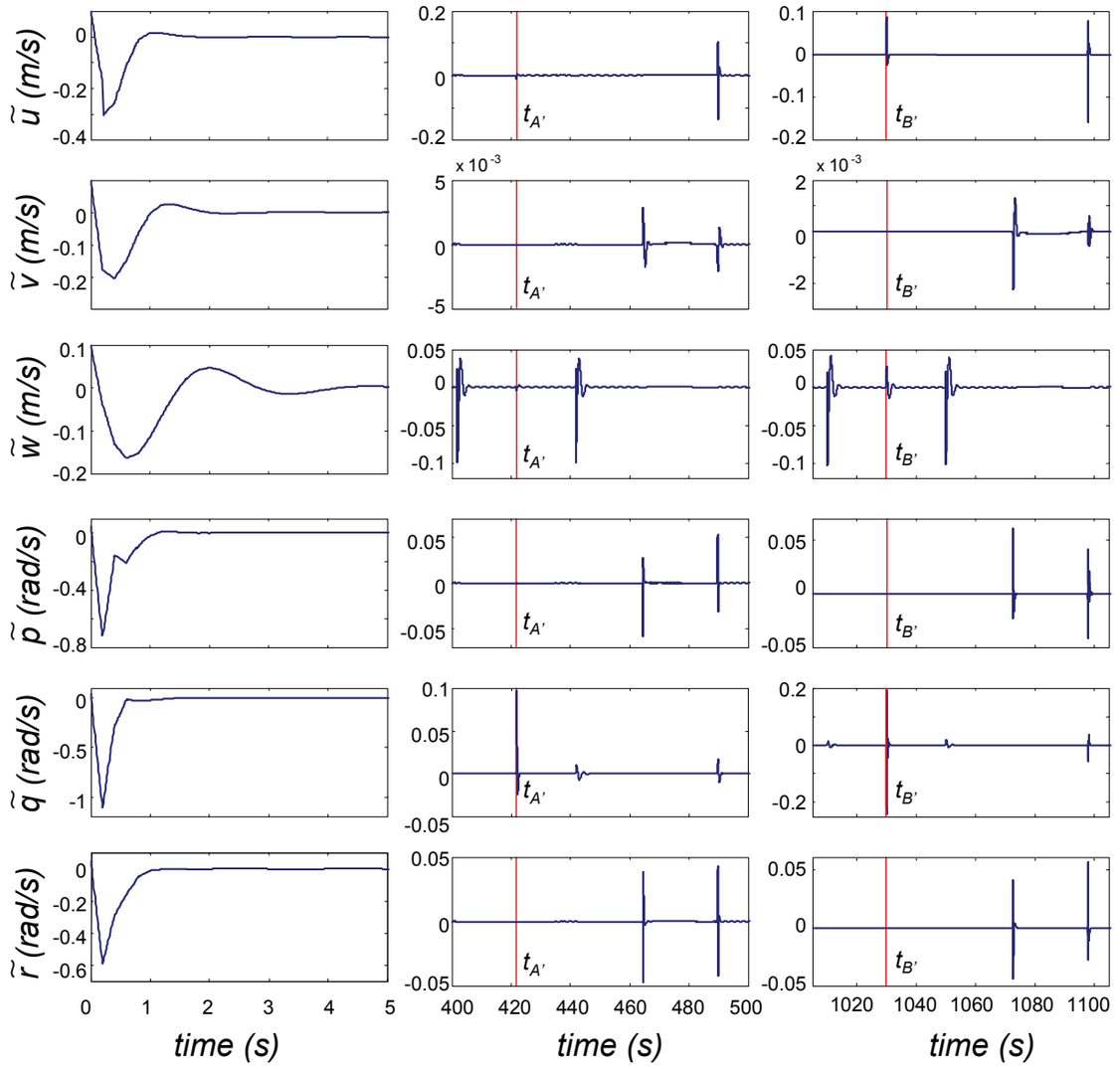

Fig. 4. Velocity path errors during transients in three different periods (from left to right column: autotuning, adaptation by weight pick up and adaptation by weight deposit)

corresponding to unmanned underwater vehicles was worked through in this work. Noisy measures as well as model uncertainties were considered by the design and analysis.

Formal proofs for stability of the digital adaptive control system and convergence of the path error trajectories were presented and an extensive analysis of the control performance was given.

It was shown that it is possible to stabilize the control loop adaptively in the six degrees of freedom without any a-priori knowledge of the vehicle system matrices with the exception of a lower bound for the inertia matrix.

Providing the noisy measures remain bounded, the adaptive controller can reduce asymptotically the path errors up to a residual set in the space state. The residual set contains the null equilibrium point and its magnitude depends on the upper bounds of the measure noises and on the sampling time. This signalizes the quality of the control performance.

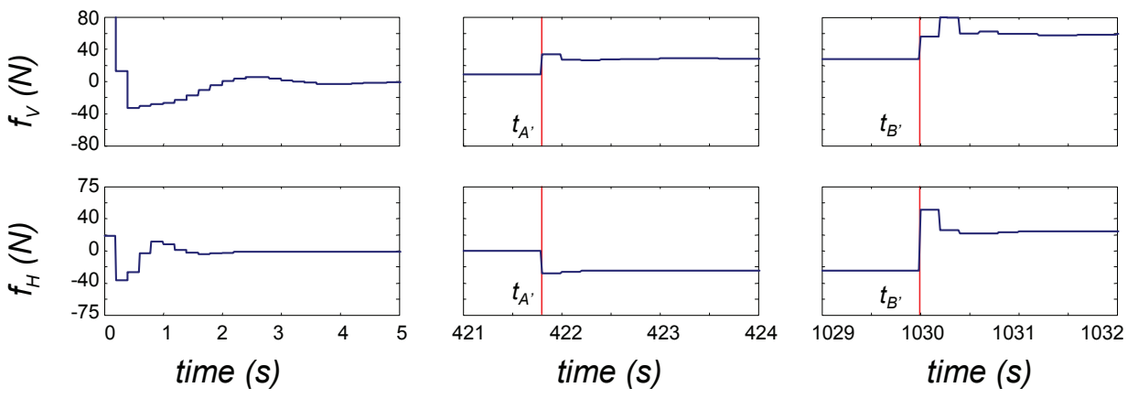

Fig. 5. Evolution of the thrust for one horizontal and one vertical thruster of the propulsion set

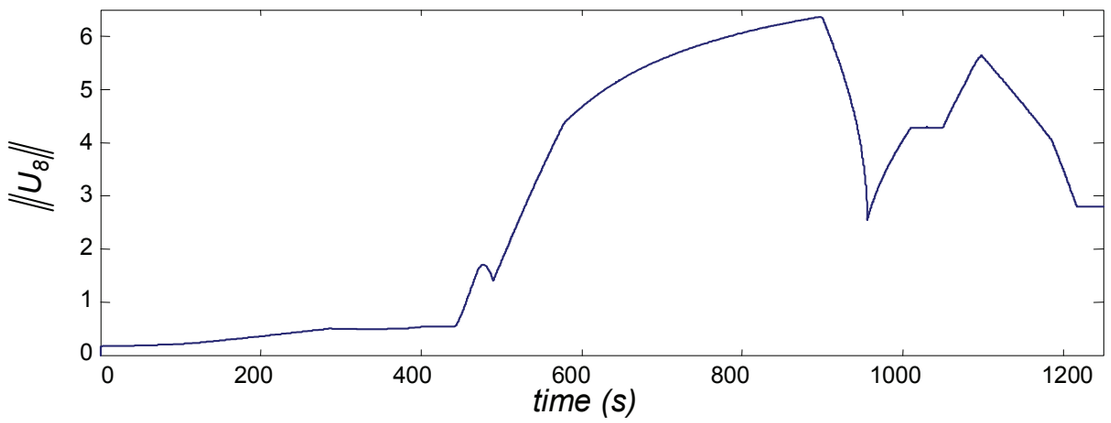

Fig. 6. Evolution of adaptive controller matrices

However, as generally occurs by digital controllers, it was observed that a large sampling time is an instabilizing factor.

It was also indicated the plausibility of obtaining a lower bound of the inertia matrix by simply calculating the inertia matrix of the body only.

We will emphasize that the design presented here was completely carried out in the discrete time domain. Other usual alternative design is the direct translation of a homologous but analog adaptive controller by digitalizing both the control and the adaptive laws. Recent results like in (Jordán & Bustamante, 2011) have shown that this alternative may lead to unstable behaviors if the sampling time is particularly not sufficiently small. This fact stands out the usefulness of our design here.

Finally, a case study was presented for an underwater vehicle in simulated sampling mission. The features of the implemented adaptive control system were highlighted by an all-round very good quality in the control performance.

9. References

[1] Antonelli, G. (2010). On the Use of Adaptive/Integral Actions for Six-Degrees-of-Freedom Control of Autonomous Underwater Vehicles, *IEEE Journal of Oceanic Engineering*. Vol. 32 (2), 300-312.

[2] Bagnell, J.A., Bradley, D., Silver, D., Sofman, B. &Stentz, A. (2010). Learning for Autonomous Navigation,
IEEE Robotics & Automation Magazine, Vol. 17(2), 74 – 84.

[3] Cunha, J.P.V.S, Costa R.R. & L. Hsu (1995). Design of a High Performance Variable Structure Position Control of ROV's, *IEEE J. of Oceanic Engineering*, Vol. 20(1), 42-55.

[4] Fossen, T.I. (1994) *Guidance and Control of Ocean Vehicles*, New York: John Wiley&Sons.

[5] Fradkov, A.L., Miroshnik, I.V. & Nikiforov, V.O. (1999). *Nonlinear and adaptive control of complex systems*, Dordrecht, The Netherlands: Kluwer Academic Publishers.

[6] Ioannou, P.A. and Sun, J. (1996). *Robust adaptive control*. PTR Prentice-Hall, Upper Saddle River, New Jersey.

[7] Inzartev , A.V. (2009)(Editor), *Underwater Vehicles*, Vienna, Austria: In-Tech.

[8] Jordán, M.A. and Bustamante, J.L. (2007) On The Presence Of Nonlinear Oscillations In The Teleoperation Of Underwater Vehicles Under The Influence Of Sea Wave And Current, *26th American Control Conference (2007 ACC)*. New York City, USA, July 11-13.

[9] Jordán, M.A. and Bustamante, J.L. (2008). Guidance Of Underwater Vehicles With Cable Tug Perturbations Under Fixed And Adaptive Control Modus, *IEEE Journal of Oceanic Engineering* , Vol. 33 (4), 579 – 598.

[10] Jordán, M.A. & Bustamante, J.L. (2009a). Adams-Bashforth Approximations for Digital Control of Complex Vehicle Dynamics, *4th Int. Scientific Conf. on Physics and Control (PHYSCON 2009)*, Catania, Italy, Sep. 1-4.

[11] Jordán, M.A. & Bustamante, J.L. (2009b). A General Approach to Sampled-Data Modeling and Digital Control of Vehicle Dynamics, 3*rd IEEE Multi-conference on Systems and Control (MSC 2009).* Saint Petersburg, Russia, July 8-10, 2009b.

[12] Jordán, M.A. and Bustamante, J.L. (2009c). *Adaptive Control for Guidance of Underwater Vehicles*, Underwater Vehicles, A.V. Inzartev (Editor), Vienna, Austria: In-Tech, Chapter 14, 251-278.

[13] Jordán, M.A. and Bustamante, J.L. (2011). An Approach to a Digital Adaptive Controller for guidance of Unmanned Vehicles - Comparison with Digitally-Translated Analog Counterparts, presented to 18th IFAC World Congress, Milan, Italia, August 29-September 2, 2011.

[14] Jordán, M.A., Bustamante, J.L. & Berger,C. (2010.) Adams-Bashforth Sampled-Data Models for Perturbed Underwater-Vehicle Dynamics, *IEEE/OES South America International Symposium*, Buenos Aires, Argentina, April 12-14.

[15] Kahveci, N.E., Ioannou, P.A. & Mirmirani, M.D. (2008). Adaptive LQ Control With Anti-Windup Augmentation to Optimize UAV Performance in Autonomous Soaring Applications, *IEEE Transactions On Control Systems Technology,* Vol. 16 (4).

[16] Krstić, M., Kanellakopoulus, I. & Kokotović, P.V. (1995). *Nonlinear and adaptive control design*. New York: John Wiley and Sons.

[17] Smallwood, D.A. & Whitcomb, L.L. (2003). Adaptive Identification of Dynamically Positioned Underwater Robotic Vehicles, *IEEE Trans. on Control Syst. Technology*, Vol. 11(4), 505-515.

[18] Sun, Y.C. & Cheah, C.C. (2003). Adaptive setpoint control for autonomous underwater vehicles, *IEEE Conf. Decision Control*, Maui, HI, Dec. 9-12.

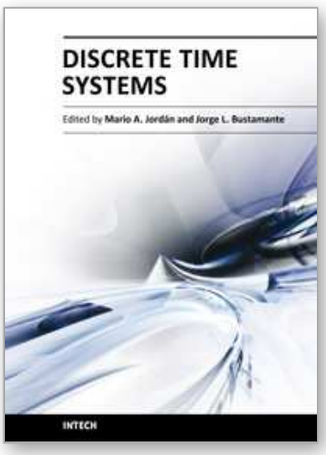

Discrete Time Systems

Edited by Dr. Mario Alberto JordÃ¡n

ISBN 978-953-307-200-5
Hard cover, 526 pages
Publisher InTech
Published online 26, April, 2011
Published in print edition April, 2011

Discrete-Time Systems comprehend an important and broad research field. The consolidation of digital-based computational means in the present, pushes a technological tool into the field with a tremendous impact in areas like Control, Signal Processing, Communications, System Modelling and related Applications. This book attempts to give a scope in the wide area of Discrete-Time Systems. Their contents are grouped conveniently in sections according to significant areas, namely Filtering, Fixed and Adaptive Control Systems, Stability Problems and Miscellaneous Applications. We think that the contribution of the book enlarges the field of the Discrete-Time Systems with signification in the present state-of-the-art. Despite the vertiginous advance in the field, we also believe that the topics described here allow us also to look through some main tendencies in the next years in the research area.

How to reference

In order to correctly reference this scholarly work, feel free to copy and paste the following:

Mario Alberto Jordán and Jorge Luis Bustamante (2011). A General Approach to Discrete-Time Adaptive Control Systems with Perturbed Measures for Complex Dynamics - Case Study: Unmanned Underwater Vehicles, Discrete Time Systems, Dr. Mario Alberto JordÃ¡n (Ed.), ISBN: 978-953-307-200-5, InTech, Available from: http://www.intechopen.com/books/discrete-time-systems/a-general-approach-to-discrete-time-adaptive-control-systems-with-perturbed-measures-for-complex-dyn

INTECH
open science | open minds

InTech Europe
University Campus STeP Ri
Slavka Krautzeka 83/A
51000 Rijeka, Croatia
Phone: +385 (51) 770 447
Fax: +385 (51) 686 166
www.intechopen.com

InTech China
Unit 405, Office Block, Hotel Equatorial Shanghai
No.65, Yan An Road (West), Shanghai, 200040, China
中国上海市延安西路65号上海国际贵都大饭店办公楼405单元
Phone: +86-21-62489820
Fax: +86-21-62489821

IntechOpen